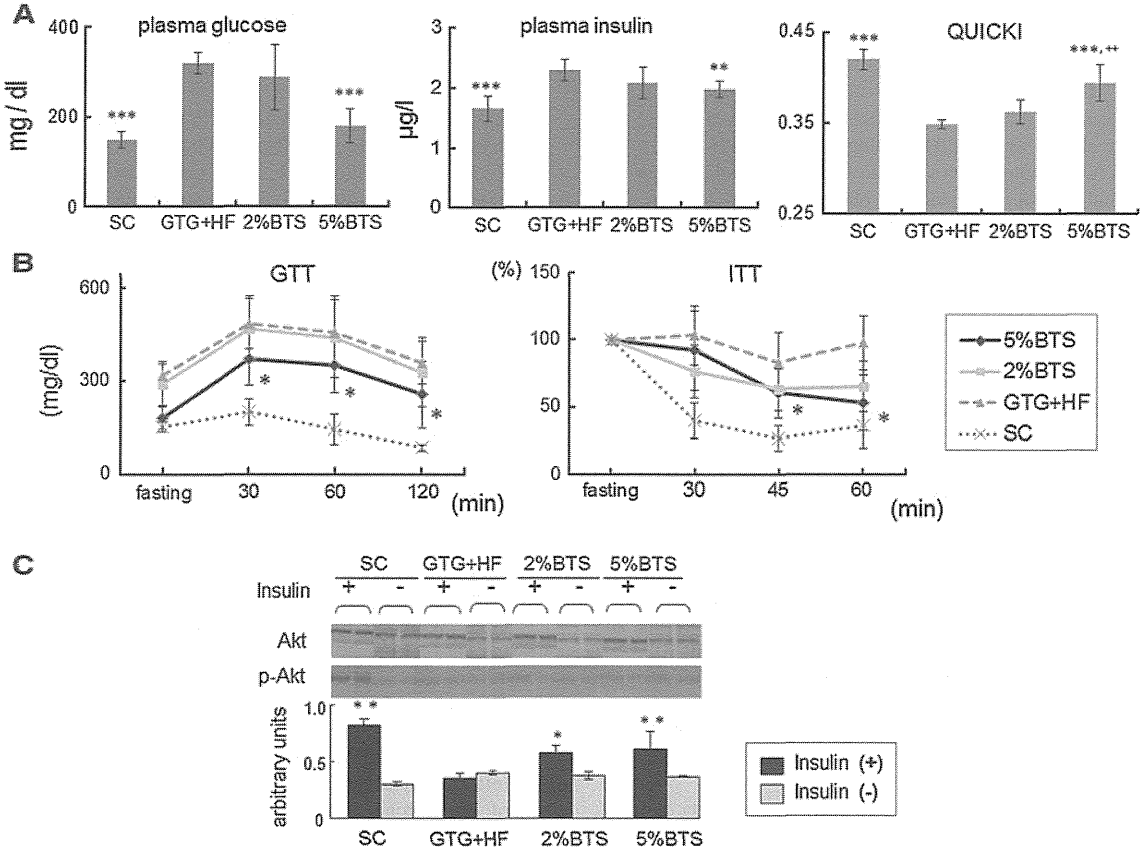

Fig. 5 Glucose intolerance and insulin resistance (IR) were attenuated by BTS. **a** Fasting plasma glucose, insulin levels and QUICKI: increased level of fasted plasma insulin and glucose were decreased, and QUICKI increased by treatment with 5 %BTS, and ITT confirmed severe IR *double asterisk* $p < 0.01$, *triple asterisk* $p < 0.001$ vs GTG + HF, *double plus symbol* $p < 0.01$ vs 2 %BTS, $n = 6$. **b** Glucose tolerance test (GTT) and insulin tolerance test (ITT): GTT revealed severe glucose intolerance was attenuated, and ITT confirmed IR was attenuated by 5 %BTS. *Asterisk* $p < 0.05$ vs GTG + HF, $n = 6$. **c** Involvement of Akt in BTS reduction of IR: phosphorylation of Akt was involved in the reduction of IR by BTS treatment as reflected by increased phosphorylation of Akt in the livers of BTS treated mice upon insulin administration. *Asterisk* $p < 0.05$, *double asterisk* $p < 0.01$ vs GTG + HF, $n = 4$

Furthermore, increased expression of DGAT2 might also have contributed to the reduction of ROS production by reducing hepatic FFA availability.

We next also investigated the effect of BTS on IR. GTG + HF induced elevation of fasting plasma glucose and plasma insulin were markedly reduced by BTS treatment, whilst QUICKI was markedly increased by BTS (Fig. 5a). In addition, ITT also was attenuated by BTS treatment. Furthermore, GTT showed that BTS remarkably attenuated severe glucose intolerance induced by GTG + HF (Fig. 5b). Phosphorylation of hepatic Akt after administration of insulin was reduced by treatment of BTS (Fig. 5c). The mechanisms through which BTS improves insulin sensitivity may involve Akt phosphorylation triggered through as yet uncertain mechanisms, but possibly involving induction of adiponectin signaling by BTS, since adiponectin is known to be involved in the suppression of hepatic gluconeogenesis and insulin secretion by activating AMPK [37].

In conclusion, therefore, BTS—a Japanese anti-obesity herbal (Kampo) medicine—is an effective preventive agent against the development of NASH. The challenge is now to identify the active components of BTS to allow its refinement and the rational design of more potent analogues.

Acknowledgments Grants-in-Aid for Scientific Research (C) 2009 Grant # 20590785, The Ministry of Education, Science, Sports and Culture, Japan (Masafumi Ono). Wellcome Trust, UK (Jude A. Oben).

Conflict of interest The authors declare that they have no conflict of interest.

References

1. Ioannou GN, Boyko EJ, Lee SP. The prevalence and predictors of elevated serum aminotransferase activity in the United States in 1999–2002. Am J Gastroenterol. 2006;101:76–82.

2. James O, Day C. Non-alcoholic steatohepatitis: another disease of affluence. Lancet. 1999;353:1634–6.
3. Guha IN, Parkes J, Roderick P, Chattopadhyay D, Cross R, Harris S, et al. Noninvasive markers of fibrosis in nonalcoholic fatty liver disease: validating the European liver fibrosis panel and exploring simple markers. Hepatology. 2008;47:455–60.
4. Hioki C, Yoshimoto K, Yoshida T. Efficacy of bofu-tsusho-san, an oriental herbal medicine, in obese Japanese women with impaired glucose tolerance. Clin Exp Pharmacol Physiol. 2004; 31:614–9.
5. Yamakawa J, Ishigaki Y, Takano F, Takahashi T, Yoshida J, Moriya J, et al. The Kampo medicines Orengedokuto, Bofutsushosan and Boiogito have different activities to regulate gene expressions in differentiated rat white adipocytes: comprehensive analysis of genetic profiles. Biol Pharm Bull. 2008;31:2083–9.
6. Shimada T, Kudo T, Akase T, Aburada M. Preventive effects of Bofutsushosan on obesity and various metabolic disorders. Biol Pharm Bull. 2008;31:1362–7.
7. Nakayama T, Suzuki S, Kudo H, Sassa S, Nomura M, Sakamoto S. Effects of three Chinese herbal medicines on plasma and liver lipids in mice fed a high-fat diet. J Ethnopharmacol. 2007;109: 236–40.
8. Sakamoto S, Takeshita S, Sassa S, Zuki S, Ishikawa Y, Kudo H. Effects of colestimide and/or Bofu-tsusho-san on plasma and liver lipids in mice fed a high-fat diet. In vivo. 2005;19:1029–33.
9. Ogasawara M, Hirose A, Ono M, Aritake K, Nozaki Y, Takahashi M, et al. A novel and comprehensive mouse model of human non-alcoholic steatohepatitis with the full range of dysmetabolic and histological abnormalities induced by gold thioglucose and a high-fat diet. Liver Int. 2011;31:542–51.
10. Oike Y, Akao M, Yasunaga K, Yamauchi T, Morisada T, Ito Y, et al. Angiopoietin-related growth factor antagonizes obesity and insulin resistance. Nat Med. 2005;11:400–8.
11. Fan W, Yanase T, Nomura M, Okabe T, Goto K, Sato T, et al. Androgen receptor null male mice develop late-onset obesity caused by decreased energy expenditure and lipolytic activity but show normal insulin sensitivity with high adiponectin secretion. Diabetes. 2005;54:1000–8.
12. Hirose A, Ono M, Saibara T, Nozaki Y, Masuda K, Yoshioka A, et al. Angiotensin II type 1 receptor blocker inhibits fibrosis in rat nonalcoholic steatohepatitis. Hepatology. 2007;45:1375–81.
13. Albrecht C, Knaapen AM, Becker A, Höhr D, Haberzettl P, van Schooten FJ, et al. The crucial role of particle surface reactivity in respirable quartz-induced reactive oxygen/nitrogen species formation and APE/Ref-1 induction in rat lung. Respir Res. 2005;6:129.
14. Guerre-Millo M, Rouault C, Poulain P, André J, Poitout V, Peters JM, et al. PPAR-alpha-null mice are protected from high-fat diet-induced insulin resistance. Diabetes. 2001;50:2809–14.
15. Ma K, Cabrero A, Saha PK, Kojima H, Li L, Chang BH, et al. Increased beta-oxidation but no insulin resistance or glucose intolerance in mice lacking adiponectin. J Biol Chem. 2002;277: 34658–61.
16. Taniguchi CM, Ueki K, Kahn R. Complementary roles of IRS-1 and IRS-2 in the hepatic regulation of metabolism. J Clin Invest. 2005;115:718–27.
17. DeBose-Boyd RA, Ou J, Goldstein JL, Brown MS. Expression of sterol regulatory element-binding protein 1c (SREBP-1c) mRNA in rat hepatoma cells requires endogenous LXR ligands. Proc Natl Acad Sci USA. 2001;98:1477–82.
18. Hui JM, Hodge A, Farrell GC, Kench JG, Kriketos A, George J. Beyond insulin resistance in NASH: TNF-alpha or adiponectin? Hepatology. 2004;40:46–54.
19. Kamada Y, Takehara T, Hayashi N. Adipocytokines and liver disease. J Gastroenterol. 2008;43:811–22.
20. Tomita K, Oike Y, Teratani T, Taguchi T, Noguchi M, Suzuki T, et al. Hepatic AdipoR2 signaling plays a protective role against progression of nonalcoholic steatohepatitis in mice. Hepatology. 2008;48:458–73.
21. Rao MS, Reddy JK. PPARalpha in the pathogenesis of fatty liver disease. Hepatology. 2004;40:783–6.
22. Reddy JK, Hashimoto T. Peroxisomal beta-oxidation and peroxisome proliferator-activated receptor alpha: an adaptive metabolic system. Annu Rev Nutr. 2001;21:193–230.
23. Namikawa C, Shu-Ping Z, Vyselaar JR, Nozaki Y, Nemoto Y, Ono M, et al. Polymorphisms of microsomal triglyceride transfer protein gene and manganese superoxide dismutase gene in non-alcoholic steatohepatitis. J Hepatol. 2004;40:781–6.
24. Yamaguchi K, Yang L, McCall S, Huang J, Yu XX, Pandey SK, et al. Inhibiting triglyceride synthesis improves hepatic steatosis but exacerbates liver damage and fibrosis in obese mice with nonalcoholic steatohepatitis. Hepatology. 2007;45:1366–74.
25. Postic C, Girard J. Contribution of de novo fatty acid synthesis to hepatic steatosis and insulin resistance: lessons from genetically engineered mice. J Clin Invest. 2008;118:829–38.
26. Whiteman EL, Cho H, Birnbaum MJ. Role of Akt/protein kinase B in metabolism. Trends Endocrinol Metab (TEM). 2002;13:444–51.
27. Kitajima Y, Eguchi Y, Ishibashi E, Nakashita S, Aoki S, Toda S, et al. Age-related fat deposition in multifidus muscle could be a marker for nonalcoholic fatty liver disease. J Gastroenterol. 2010; 45:218–24.
28. Tsuchida A, Yamauchi T, Takekawa S, Hada Y, Ito Y, Maki T, et al. Peroxisome proliferator-activated receptor (PPAR)alpha activation increases adiponectin receptors and reduces obesity-related inflammation in adipose tissue: comparison of activation of PPARalpha, PPARgamma, and their combination. Diabetes. 2005;54:3358–70.
29. Waki H, Yamauchi T, Kamon J, Ito Y, Uchida S, Kita S, et al. Impaired multimerization of human adiponectin mutants associated with diabetes. Molecular structure and multimer formation of adiponectin. J Biol Chem. 2003;278:40352–63.
30. Shklyaev S, Aslanidi G, Tennant M, Prima V, Kohlbrenner E, Kroutov V, et al. Sustained peripheral expression of transgene adiponectin offsets the development of diet-induced obesity in rats. Proc Natl Acad Sci USA. 2003;100:14217–22.
31. Browning JD, Horton JD. Molecular mediators of hepatic steatosis and liver injury. J Clin Invest. 2004;114:147–52.
32. Yamauchi T, Nio Y, Maki T, Kobayashi M, Takazawa T, Iwabu M, et al. Targeted disruption of AdipoR1 and AdipoR2 causes abrogation of adiponectin binding and metabolic actions. Nat Med. 2007;13:332–9.
33. Yano W, Kubota N, Itoh S, Kubota T, Awazawa M, Moroi M, et al. Molecular mechanism of moderate insulin resistance in adiponectin-knockout mice. Endocr J. 2008;55:515–22.
34. Endo M, Masaki T, Seike M, Yoshimatsu H. TNF-alpha induces hepatic steatosis in mice by enhancing gene expression of sterol regulatory element binding protein-1c (SREBP-1c). Exp Biol Med (Maywood). 2007;232:614–21.
35. Evans JL, Goldfine ID, Maddux BA, Grodsky GM. Are oxidative stress-activated signaling pathways mediators of insulin resistance and beta-cell dysfunction? Diabetes. 2003;52:1–8.
36. Leclercq IA, Farrell GC, Field J, Bell DR, Gonzalez FJ, Robertson GR. CYP2E1 and CYP4A as microsomal catalysts of lipid peroxides in murine nonalcoholic steatohepatitis. J Clin Invest. 2000;105:1067–75.
37. Yamauchi T, Kamon J, Minokoshi Y, Ito Y, Waki H, Uchida S, et al. Adiponectin stimulates glucose utilization and fatty-acid oxidation by activating AMP-activated protein kinase. Nat Med. 2002;8:1288–95.

PLOS ONE

Glycemic Variability Is an Independent Predictive Factor for Development of Hepatic Fibrosis in Nonalcoholic Fatty Liver Disease

Motoi Hashiba[1], Masafumi Ono[1]*, Hideyuki Hyogo[2], Yukio Ikeda[3], Kosei Masuda[1], Reiko Yoshioka[1], Yoichi Ishikawa[1], Yuri Nagata[1], Kensuke Munekage[1], Tsunehiro Ochi[1], Akira Hirose[1], Yasuko Nozaki-Fujimura[1], Shuhei Noguchi[4], Nobuto Okamoto[1], Kazuaki Chayama[2], Narufumi Suganuma[4], Toshiji Saibara[1]

1 Department of Gastroenterology and Hepatology, Kochi Medical School, Kochi, Japan, **2** Department of Medicine and Molecular Science, Graduate School of Biomedical Sciences, Hiroshima University, Hiroshima, Japan, **3** Diabetes Center, Kochi Memorial Hospital, Kochi, Japan, **4** Department of Environmental Medicine, Kochi Medical School, Kochi, Japan

Abstract

Patients with nonalcoholic fatty liver disease (NAFLD) and nonalcoholic steatohepatitis (NASH) often have metabolic disorders including insulin resistance and type 2 diabetes mellitus (T2DM). We clarified the predictive factors in glucose metabolism for progression of hepatic fibrosis in patients with NAFLD by the 75-g oral glucose tolerance test (75gOGTT) and a continuous glucose monitoring system (CGMS). One hundred sixty-nine patients (68 female and 101 male patients) with biopsy-proven NAFLD with performance with 75gOGTT were enrolled and divided into four groups according to the stage of hepatic fibrosis (F0–3). The proportion of patients with T2DM significantly gradually increased, HbA1c and the homeostasis model assessment of insulin resistance were significantly elevated, and 1,5-anhydroglucitol (1,5-AG) was remarkably decreased with the progression of fibrosis. In the 75gOGTT, both plasma glucose and insulin secretion were remarkably increased with the progression of fibrosis. The only factor significantly associated with advanced fibrosis was 1,5-AG ($P=0.008$) as determined by multivariate logistic regression analysis. We next evaluated the changes in blood glucose during 24 hours by monitoring with the CGMS to confirm the relationship between glycemic variability and progression of fibrosis. Variability of median glucose, standard deviation of median glucose ($P=0.0022$), maximum blood glucose ($P=0.0019$), and ΔMin–max blood glucose ($P=0.0029$) were remarkably higher in severe fibrosis than in mild fibrosis.

Conclusion: Hyperinsulinemia and hyperglycemia, especially glycemic variability, are important predictive factors in glucose impairment for the progression of hepatic fibrosis in NAFLD.

Citation: Hashiba M, Ono M, Hyogo H, Ikeda Y, Masuda K, et al. (2013) Glycemic Variability Is an Independent Predictive Factor for Development of Hepatic Fibrosis in Nonalcoholic Fatty Liver Disease. PLoS ONE 8(11): e76161. doi:10.1371/journal.pone.0076161

Editor: Manlio Vinciguerra, University College London, United Kingdom

Received July 2, 2013; **Accepted** August 20, 2013; **Published** November 6, 2013

Funding: This work was supported by Grants-in-Aid for Scientific Research (C) 2011 Grant # 23590979, Ministry of Education, Culture, Sports, Science and Technology, Japan. The funders had no role in study design, data collection and analysis, decision to publish, or preparation of the manuscript.

Competing Interests: The authors have declared that no competing interests exist.

* E-mail: onom@kochi-u.ac.jp

Introduction

Nonalcoholic fatty liver disease (NAFLD) includes a wide spectrum of liver diseases that range from simple steatosis, which is usually a benign and non-progressive condition, to nonalcoholic steatohepatitis (NASH), which can progress to liver cirrhosis (LC) and hepatocellular carcinoma in the absence of significant alcohol consumption [1–3]. The progression of hepatic fibrosis is an important predictive factor for the development of LC and hepatocellular carcinoma not only in patients with chronic hepatitis C, but also in those with NASH [4]. To inhibit the progression of hepatic fibrosis in NASH, it is important to clarify the predictive factors for progression of hepatic fibrosis.

NASH and NAFLD are considered to be hepatic manifestations of the metabolic syndrome including insulin resistance (IR) and abnormalities of glucose metabolism [5,6]. In accordance with the increased prevalence of obesity and type 2 diabetes mellitus (T2DM) in the general population worldwide, the number of patients with NASH and NAFLD have also increased [7,8]. T2DM is considered to be an independent risk factor for the development of NASH and NAFLD [9,10], and hyperinsulinemia and hyperglycemia are common not only in obese patients, but also in non-obese, non-diabetic patients with NASH [11]. On the other hand, the presence of NASH and NAFLD themselves is also considered to be associated with a high risk of developing T2DM [12].

Postprandial hyperglycemia and glycemic variability were reported to involve progression of atherosclerosis through increase of oxidative stress, activation of inflammatory cytokines and inflammation [13–15]. Oxidative stress is well known as one of most important factor for inflammation and progression of hepatic fibrosis in NAFLD patients [16,17]. The continuous glucose

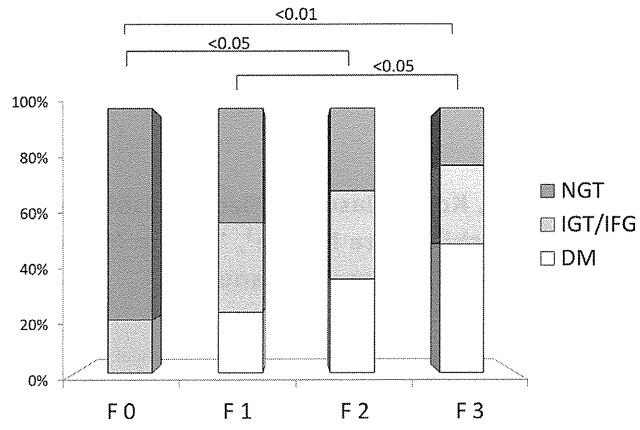

Figure 1. Relationship between glucose impairment and progression of hepatic fibrosis. The frequencies of NGT, IGT/IFG, and T2DM in the four stages of hepatic fibrosis are shown. The diagnosis of glucose impairment was based on the 75gOGTT. The prevalence of NGT in patients in the F0 group (80.0%) was significantly higher than that in the F1 (43.2%), F2 (31.3%), and F3 groups (21.6%), and the frequencies of patients with T2DM in the F3 group (48.6%) was significantly higher than that in the F0 (0%), F1 (22.9%), and F2 (35.4%) groups. *P*-values were calculated using the X^2-test. Fibrosis stage (F): F0 ($n=10$), F1 ($n=74$), F2 ($n=48$), F3 ($n=37$); total, N = 169.
doi:10.1371/journal.pone.0076161.g001

monitoring system (CGMS) has been introduced as a useful tool, which detect postprandial hyperglycemia [18] and glycemic variability during 24 hours in DM patients. In addition, episodic hypoglycemia during sleeping time can also be detected by CGMS [19]. However, postprandial hyperglycemia and glycemic variability have not yet been evaluated by CGMS in NAFLD patients. Moreover, the relationship between the clinical features of glucose impairment and the progression of hepatic fibrosis in NASH and NAFLD has not been well elucidated. In this study, therefore, we clarified the predictive factors in glucose metabolism for the progression of hepatic fibrosis in NAFLD using the 75-g oral glucose tolerance test (75gOGTT) and CGMS.

Patients and Methods

Patients

A total of 169 patients with biopsy-proven NAFLD (68 female and 101 male patients) with performance with 75gOGTT were enrolled in this study. Liver biopsies had been obtained in all patients after a thorough clinical evaluation had been performed and signed informed consent had been obtained from each patient. Patients with known use of methotrexate, tamoxifen, corticosteroids, or alcohol in excess of 20 g per day and patients with other known causes of liver disease including viral hepatitis, hemochromatosis, Wilson's disease, and autoimmune liver diseases were excluded from this study. None of the patients had received anti-diabetic drugs or insulin. The study protocol conformed to the ethical guidelines of the 1975 Declaration of Helsinki [20] and was approved by the Research Committee of Kochi Medical School.

Clinical and Laboratory Evaluation

Venous blood samples were obtained in the morning after a 12-hour overnight fast. Laboratory tests in all patients included measurements of serum aspartate aminotransferase, alanine aminotransferase, gamma-glutamyl transpeptidase, lipid profiles, total cholesterol, triglycerides, high-density lipoprotein cholesterol, low-density lipoprotein cholesterol, fasting plasma glucose, fasting immunoreactive insulin (f-IRI), creatinine, blood urea nitrogen, 1,5-anhydroglucitol (1,5-AG), HbA1c, and fibrosis markers. These parameters were measured using standard clinical chemistry techniques in the laboratory section of Kochi Medical School Hospital. All patients underwent the 75gOGTT. Plasma glucose and insulin concentrations were measured at 0, 30, 60, 90, 120, and 180 minutes. Insulin resistance was calculated by the homeostasis model (HOMA)-IR using following formula: HOMA-IR = fasting plasma insulin (μU/ml) X fasting plasma glucose (mg/dl)/405. The measure of insulin secretion was calculated by the insulinogenic index using following formula: insulinogenic index = (Δplasma insulin 0–30 min)/(Δplasma glucose 0–30 min).

Histological Evaluation

Liver biopsies of all patients were performed percutaneously under ultrasonographic guidance, and biopsy specimens were obtained from the liver parenchyma of the upper region of the right lobe using a 15-gauge biopsy needle. Liver biopsy specimens were routinely fixed in 10% phosphate-buffered formalin (pH 7.4), embedded in paraffin, and sectioned for hematoxylin and eosin staining. Hepatic fibrosis was assessed by Brunt's classification [21], and fibrosis staging was as follows: 0 = no fibrosis; 1 = zone 3 fibrosis only; 2 = zone 3 and portal/periportal fibrosis; 3 = bridging fibrosis; and 4 = cirrhosis. Histological evaluation was performed by two pathologists with no knowledge of the patients' clinical data.

Continuous Glucose Monitoring System (CGMS)

Continuous glucose levels in 20 patients with biopsy-proven NAFLD were monitored by the CGMS System Gold (Medtronic MiniMed, Northridge, CA, USA). None of the patients had received anti-diabetic drugs, including insulin injection. In the severe hepatic fibrosis group, four patients with NAFLD with F4 fibrosis (LC) were included in this study, unlike in the 75gOGTT study. According to the operating guidelines, the CGMS was installed in the patients to monitor the glucose levels of interstitial fluid [22]. The glucose sensor was inserted into the subcutaneous tissue of the abdomen at 3:00 to 4:00 PM and was monitored for 30 hours. Finger-stick blood glucose levels were checked to calibrate the first glucose value of the CGMS after 1 hour of initialization. Glucose concentrations were determined at least four times per day with an automatic blood glucose meter (Glutest; Sanwa Kagaku Kenkyusho Co., Ltd., Nagoya, Japan). Meals were strictly standardized (1800 kcal/day of standard diets at Kochi Medical School Hospital) during the examination.

Statistical Analyses

Results are presented as mean ± standard deviation for quantitative data and as numbers or percentages for categorical or qualitative data. Statistical differences in quantitative data were determined using the Mann-Whitney U test or post-hoc test. Qualitative data were compared using the chi-square test. Multivariate analysis was carried out by logistic regression. These statistical analyses were carried out using Small Stata 10.1 for Windows. Results were considered significant when the P value was <0.05.

Results

Relationship between glucose impairment and progression of hepatic fibrosis

To investigate the relationship among clinical features of glucose levels, insulin secretion, and hepatic fibrosis, the 169

Table 1. Clinical and physiological characteristics of patients with NAFLD in the four stages of hepatic fibrosis.

	F0 (n = 10)			F1 (n = 74)			F2 (n = 48)			F3 (n = 37)		
Gender (F/M)	**4/6**			**25/49**			**18/30**			**21/16**		
Age (yo)	39.6	±	12.2	45.6	±	15.4	49.1	±	14.2	53.6	±	14.3*** ,##
BMI (kg/m^2)	27.4	±	3.0	27.6	±	5.5	28.3	±	4.3	30.1	±	4.6 ##
AST (IU/L)	37.8	±	11.1	43.4	±	20.9	54.5	±	32.8 #	79.3	±	46.1**,###, ++
ALT (IU/L)	64.5	±	29.4	78.2	±	37.1	99.8	±	67.6 #	111.1	±	68.1*, #
ALP (IU/L)	207.2	±	109.9	240.8	±	109.8	287.8	±	100.7	253.1	±	106.3
GGT (IU/L)	113.6	±	101.3	58.2	±	42.9 **	79.7	±	40.0	91.8	±	80.3 #
ChE (IU/L)	375.9	±	59.2	359.8	±	77.7	371.5	±	54.8	328.0	±	82.6
Albumin (g/dl)	4.44	±	0.22	4.58	±	0.28	4.45	±	0.28	4.45	±	0.31
BUN (mg/dl)	13.8	±	2.6	13.8	±	4.0	14.8	±	4.9	13.7	±	3.9
Crn (mg/dl)	0.69	±	0.11	0.84	±	0.97	0.66	±	0.22	0.68	±	0.12
UA (mg/dl)	6.38	±	1.70	6.42	±	2.21	6.38	±	1.29	5.85	±	1.08
FPG (mg/dl)	90.8	±	8.6	104.6	±	24.1	100.6	±	15.5	106.5	±	20.9 *
HbA1c (%)	5.46	±	0.22	5.92	±	1.14	5.96	±	0.77 *	6.27	±	0.98 *
T-Cho (mg/dl)	214.6	±	39.8	203.5	±	35.3	222.2	±	29.8 #	215.3	±	53.7 +
TG (mg/dl)	185.9	±	144.9	150.4	±	90.6	186.8	±	98.0 #	142.7	±	55.0 +
RBC (×10^4/ml)	467.0	±	49.5	478.9	±	49.0	446.4	±	38.9	445.1	±	38.2 #
Hb (g/dl)	14.1	±	1.4	14.3	±	1.8	13.9	±	1.6	13.9	±	0.8
Plt (×10^4/ml)	24.0	±	5.3	23.7	±	5.9	22.8	±	3.8 #	20.0	±	5.4 # #
WBC (×10^3/ml)	4.47	±	3.18	5.29	±	2.54	5.42	±	2.64	4.02	±	3.10
Fe (mg/dl)	93.2	±	17.6	106.4	±	30.6	107.2	±	20.6	127.1	±	42.6 #
Ferritin (ng/ml)	155.7	±	131.0	241.7	±	172.9	262.9	±	192.6	328.3	±	277.2 #
HA (ng/ml)	20.2	±	13.5	30.4	±	19.5	34.1	±	26.3	93.5	±	105.0 ###, +++
IVcollagen7S (ng/ml)	2.79	±	0.52	3.52	±	0.67 **	3.77	±	1.01 **	5.05	±	2.35*,###, ++
P-3-P (U/ml)	0.53	±	0.14	0.57	±	0.17	0.69	±	0.24	0.92	±	0.66 #

P-values were calculated using the Mann–Whitney U test. Versus F0: *P<0.05, **P<0.01, ***P<0.001. Versus F1: #P<0.05, ##P<0.01, ###P<0.001. Versus F2: ++P<0.01, +++P<0.001. Fibrosis stage (F): F0 (n = 10), F1 (n = 74), F2 (n = 48), F3 (n = 37); total, N = 169. BMI, body mass index; AST, aspartate aminotransferase; ALT, alanine aminotransferase; GGT, gamma-glutamyl transpeptidase; ChE, cholinesterase; UA, uric acid; T-Cho, total cholesterol; TG, triglycerides; FPG, fasting plasma glucose; Plt, platelets; Fe, plasma iron; HA, hyaluronic acid; IV collagen 7S, type IV collagen 7S; P-3-P, type III procollagen N-peptide.

doi:10.1371/journal.pone.0076161.t001

patients with NAFLD were classified into four groups based on the stage of hepatic fibrosis stage: F0 ($n = 10$), F1 ($n = 74$), F2 ($n = 48$), and F3 ($n = 37$). The clinical and physiological data of the four groups are shown in Table 1. The hepatic fibrosis markers hyaluronic acid, type IV collagen 7S, and type III procollagen N-peptide were significantly increased according to the progression of hepatic fibrosis. In addition, the patients with severe fibrosis were much older and had higher ferritin and transaminase levels. The platelet count tended to decrease according to the progression of hepatic fibrosis. We next evaluated the relationship between the prevalence of T2DM diagnosed by 75gOGTT and the stage of hepatic fibrosis in patients with NAFLD. The prevalence of patients with normal glucose tolerance (NGT) was 80%, and no patients with T2DM were found in the F0 group (Fig. 1). On the other hand, the prevalence of NGT in the patients with F3 disease was only 21.6%, and the prevalence of T2DM was 48.6%. In accordance with the progression of hepatic fibrosis, the prevalence of patients with T2DM was significantly gradually increased (F0 versus F2, $P<0.05$; F0 versus F3, $P<0.01$; F1 versus F3, $P<0.05$). To clarify the factors of glucose impairment that are related to the progression of hepatic fibrosis, we evaluated the various parameters of glucose metabolism.

Figure 2A shows that the patients with advanced hepatic fibrosis showed significantly higher levels of HbA1c (F0 versus F2, $P<0.05$; F0 versus F3, $P<0.05$). In addition, 1,5-AG was significantly decreased in accordance with the progression of hepatic fibrosis (F0 versus F2, $P<0.05$; F0 versus F3, $P<0.0001$; F1 versus F3, $P<0.001$; F2 versus F3, $P<0.05$) (Fig. 2B). Severe variability of plasma glucose levels might involve the progression of hepatic fibrosis. HOMA-IR was also elevated in the patients with advanced hepatic fibrosis (F0 versus F2, $P<0.05$; F0 versus F3, $P<0.05$; F1 versus F2, $P<0.05$; F1 versus F3, $P<0.01$) (Fig. 2C). On the other hand, although the insulinogenic index tended to decrease in accordance with the progression of hepatic fibrosis, no statistically significant difference was recognized in our study (Fig. 2D).

We next evaluated the patterns of glucose and insulin secretion by the 75gOGTT in patients with NAFLD. As shown in Figure 3A, not only the fasting glucose levels (F0 versus F3, $P<0.05$), but also the glucose levels after oral glucose loading (at 30, 60, 90, and 120 minutes) were significantly increased in parallel with the progression of fibrosis. The area under the curve (AUC) of the plasma glucose level (AUC-PG) as the marker for total glucose secretion after oral glucose loading also increased in accordance with the progression of hepatic fibrosis (F0 versus F2, $P<0.05$; F0

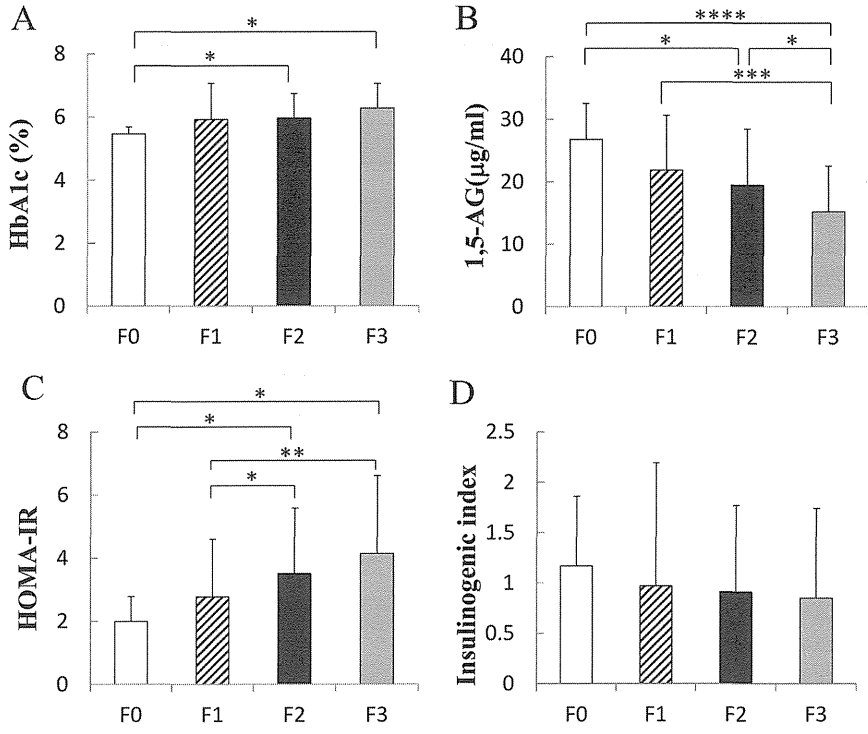

Figure 2. Relationship between hepatic fibrosis and various parameters of glucose metabolism. A) HbA1c was significantly elevated in accordance with the progression of hepatic fibrosis (F0 versus F2, *$P<0.05$; F0 versus F3, **$P<0.05$; N = 169). B) 1,5-Anhydroglucitol (1,5-AG) levels were remarkably decreased with the progression of hepatic fibrosis (F0 versus F2, *$P<0.05$; F0 versus F3, ****$P<0.0001$; F1 versus F3, ***$P<0.001$; F2 versus F3, *$P<0.05$; N = 169). C) HOMA-IR was significantly elevated in the patients with advanced hepatic fibrosis (F0 versus F2, *$P<0.05$; F0 versus F3, *$P<0.05$; F1 versus F2, *$P<0.05$; F1 versus F3, **$P<0.01$; N = 169). D) The insulinogenic index did not differ among the fibrosis groups (N = 169).
doi:10.1371/journal.pone.0076161.g002

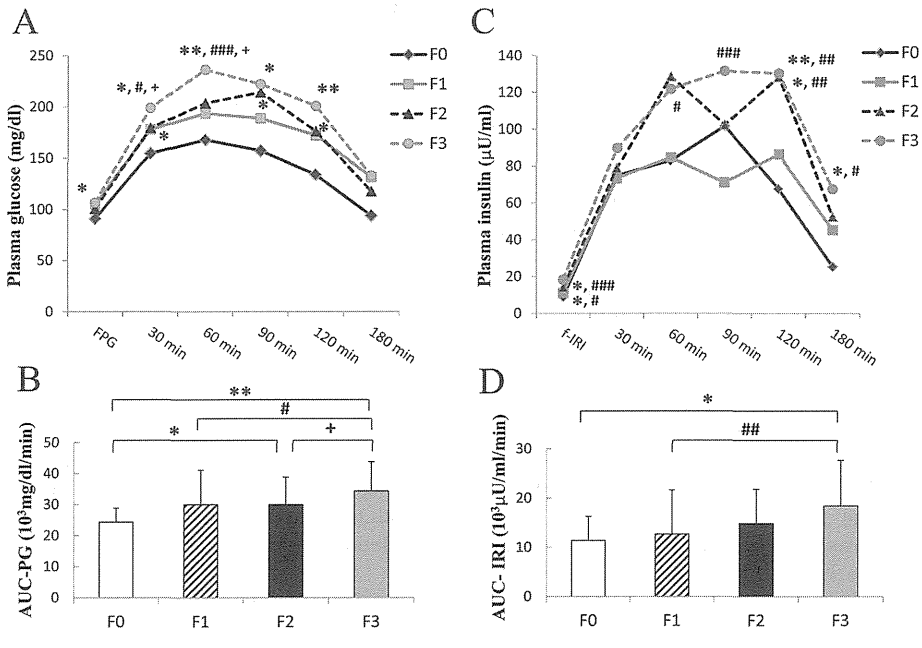

Figure 3. Patterns of glucose and insulin secretion in the 75gOGTT in relation to the progression of hepatic fibrosis. A) The glucose levels were significantly elevated in accordance with the progression of fibrosis (Versus F0: *$P<0.05$, **$P<0.01$; Versus F1: $^{\#}P<0.05$, $^{\#\#\#}P<0.001$; Versus F2: $^{+}P<0.05$). B) Area under the curve (AUC) of plasma glucose levels (AUC-PG) was remarkably larger in accordance with the progression of hepatic fibrosis (F0 versus F2, *$P<0.05$; F0 versus F3, **$P<0.01$; F1 versus F3, $^{\#}P<0.05$; F2 versus F3, $^{+}P<0.05$) C) Insulin secretion levels were remarkably higher in the patients with progression of hepatic fibrosis (Versus F0: *$P<0.05$, **$P<0.01$; Versus F1: $^{\#}P<0.05$, $^{\#\#}P<0.01$, $^{\#\#\#}P<0.001$). D) AUC of insulin secretion (AUC-IRI) was also significantly larger in accordance with the progression of hepatic fibrosis (F0 versus F3, *$P<0.05$; F1 versus F3, $^{\#\#}P<0.01$). (Black diamond: F0: n = 10. Gray square: F1: n = 74. Black triangle: F2: n = 48. Gray circle: F3: n = 37; total, N = 169).
doi:10.1371/journal.pone.0076161.g003

Table 2. Comparison of the parameters of glucose metabolism between patients with mild fibrosis (F0–2) and severe fibrosis (F3).

	F0-2		F3		P value
	(n = 132)		(n = 37)		
Gender (F/M)	**47/85**		**21/16**		
Age (yo)	46.4	± 14.9	53.6	± 14.3	0.00967
BMI (kg/m^2)	27.4	± 3.0	30.1	± 4.6	0.01395
FPG (mg/dl)	102.1	± 20.7	106.5	± 20.9	0.25665
HbA1c (%)	5.90	± 0.97	6.27	± 0.98	0.04520
f-IRI (μU/ml)	12.0	± 7.5	18.3	± 11.8	0.00012
HOMA-IR	2.98	± 1.92	4.14	± 2.47	0.00320
insulinogenic index	0.96	± 1.06	0.85	± 0.89	0.54574
AUC-IRI (10^3μU/ml/min)	12.9	± 8.3	18.4	± 9.2	0.00103
AUC-PG (10^3mg/dl/min)	29.6	± 10.0	34.3	± 9.5	0.01093
1,5-AG (μg/ml)	21.4	± 8.8	15.2	± 7.3	0.00014

P-values were calculated using the Mann–Whitney U test. Data are expressed as mean ± standard deviation. BMI, body mass index; FPG, fasting plasma glucose; f-IRI, fasting immunoreactive insulin; HOMA-IR, homeostasis model assessment of insulin resistance; AUC-IRI, area under the curve of IRI secretion; AUC-PG, area under the curve of plasma glucose; 1,5-AG, 1,5-anhydroglucitol.
doi:10.1371/journal.pone.0076161.t002

versus F3, $P<0.01$; F1 versus F3, $P<0.05$; F2 versus F3, $P<0.05$) (Fig. 3B). In addition, f-IRI was significantly elevated in accordance with the progression of hepatic fibrosis (F0 versus F2, $P<0.05$; F0 versus F3, $P<0.05$; F1 versus F2, $P<0.05$; F1 versus F3, $P<0.001$) (Fig. 3C). Furthermore, the AUC of IRI secretion (AUC-IRI) was also significantly increased in accordance with the progression of hepatic fibrosis (F0 versus F3, $P<0.05$; F1 versus F3, $P<0.01$) (Fig. 3D). In particular, the insulin levels at 120 minutes were remarkably higher in the patients with advanced hepatic fibrosis (F0 versus F2, $P<0.05$; F0 versus F3, $P<0.01$; F1 versus F2, $P<0.01$; F1 versus F3, $P<0.01$). On the other hand, insulin secretion levels at 30 minutes were not statistically different among the groups.

To clarify the prognostic factors associated with advanced hepatic fibrosis, the factors that might be related to glucose metabolism were compared between the mild fibrosis group (F0–2) and severe fibrosis group (F3). Table 2 shows that age, body mass index, HbA1c, f-IRI, HOMA-IR, AUC-IRI, and AUC-PG were significantly higher in the F3 group than in the F0–2 group. Furthermore, 1,5-AG was significantly lower in the F3 group than in the F0–2 group ($P = 0.00014$). In contrast, fasting plasma glucose and the insulinogenic index were not significantly different between these groups. As determined by multivariate logistic regression analysis, 1,5-AG ($P = 0.008$; Z value, -2.65; odds ratio [OR], 0.89509; 95% confidence interval [CI], 0.82473–0.97145) was the only independent factor for association of advanced hepatic fibrosis in patients with NAFLD (Table 3).

Table 3. Factors associated with progression of hepatic fibrosis in multivariate logistic regression analysis.

	Odds ratio	95% CI	Z value	P value
Age (yo)	1.04252	1.00009–1.08676	1.96	0.051
BMI (kg/m^2)	1.08810	0.96010–1.23318	1.32	0.186
HbA1c (%)	0.82385	0.37798–1.79568	−0.49	0.626
f-IRI (μU/ml)	1.15005	0.89106–1.48432	1.07	0.283
HOMA-IR	0.81485	0.32819–2.02311	−0.44	0.659
insulinogenic index	0.59433	0.29955–1.17917	−1.49	0.137
AUC-IRI (10^3μU/ml/min)	1.00006	0.99997–1.00014	1.29	0.196
AUC-PG (10^3mg/dl/min)	1.00000	0.99989–1.00011	−0.08	0.937
1,5-AG (μg/ml)	0.89509	0.82473–0.97145	−2.65	0.008

P-values were calculated using logistic regression. BMI, body mass index; FPG, fasting plasma glucose; f-IRI, fasting immunoreactive insulin; HOMA-IR, homeostasis model assessment of insulin resistance; AUC-IRI: area under the curve of IRI secretion; AUC-PG, area under the curve of plasma glucose; 1,5-AG, 1,5-anhydroglucitol; CI, confidence interval.
doi:10.1371/journal.pone.0076161.t003

Continuous glucose monitoring system (CGMS) clarified that variability of glucose changes was associated with advanced hepatic fibrosis

In multivariate logistic regression analysis, 1,5-AG was selected as the independent associated factor for advanced hepatic fibrosis. A lower 1,5-AG might indicate not only poor control of plasma glucose, but also severe variability of plasma glucose changes. We hypothesized that severe variability of plasma glucose levels might involve the progression of hepatic fibrosis. To address our hypothesis, we investigated the variability of glucose levels during 24 hours by a CGMS. We used the CGMS for 10 patients in the severe fibrosis group (F3–4), including patients with LC, and 10 patients in the mild hepatic fibrosis group (F0–2). No patients in either group took any anti-diabetes drugs or insulin injections. The clinical data of both groups are shown in Table S1 in File S1.

The average median glucose level of the patients with mild fibrosis (F0–2) was significantly lower than that in the patients with severe fibrosis (F3–4) (108.1±12.1 versus 132.8±39.5 mg/dl, $P<0.00001$) (Fig. 4 and Table 4). The variability of median glucose levels of the patients with mild fibrosis was remarkably smaller than that in the patients with severe fibrosis, as shown in Figure 4. The standard deviation of the median glucose levels in the patients with mild fibrosis was remarkably smaller than that in the patients with severe fibrosis (17.4±5.2 versus 39.7±17.8 mg/dl, $P = 0.0022$). In addition, ΔMin–max blood glucose was also significantly larger in patients with severe fibrosis than in those with mild fibrosis (165.0±69.6 versus 115.2±22.8 mg/dl, $P = 0.0029$). Furthermore, all postprandial glucose levels (shadowed areas in Fig. 4, from $P<0.05$ to $P<0.001$) and maximum glucose levels ($P = 0.0019$) (Table 4) in the patients with severe fibrosis were significantly higher than those in the patients with mild fibrosis, although the minimum blood glucose levels were not significantly different ($P = 0.9221$).

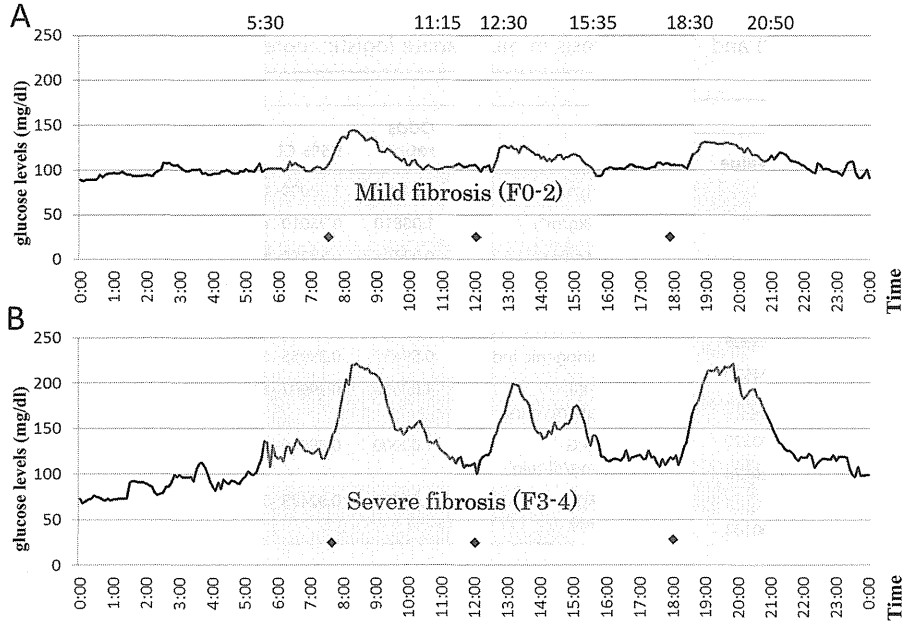

Figure 4. Twenty-four-hour sensor glucose profiles by continuous glucose monitoring system. The changes in the median sensor glucose levels during 24 hours are shown in the patients with A) mild fibrosis (F0–2, $n=10$) and B) severe fibrosis (F3–4, $n=10$). The variability of median glucose levels among the patients with mild fibrosis was remarkably smaller than that among the patients with severe fibrosis. Median glucose levels in the patients with severe fibrosis were higher than those with mild fibrosis (shadows areas, $P<0.05$ to $P<0.001$). Black diamond: Time of meal consumption.
doi:10.1371/journal.pone.0076161.g004

Discussion

The number of patients with NAFLD and NASH has increased according to the increase in the prevalence of patients with obesity and T2DM worldwide. Patients with NAFLD and NASH often have metabolic disorders including IR and T2DM. In particular, IR is considered to be one of most important background factors for the development of NAFLD and NASH. However, detailed clinical features of impairment of glucose metabolism in patients with NAFLD and NASH are not well understood. In this study, we clarified the predictive factors in glucose metabolism for the development of hepatic fibrosis in patients with NAFLD by the 75gOGTT and CGMS methods.

We evaluated the relationship between the prevalence of T2DM diagnosed by the 75gOGTT and the degree of hepatic fibrosis in patients with NAFLD (Fig. 1). No patients with F0 fibrosis had T2DM, but 80% had NGT. On the other hand, the prevalence of NGT in the patients with F3 fibrosis was only 21.6%, and the prevalence of T2DM was 48.6%. In accordance with the progression of hepatic fibrosis, the prevalence of patients with T2DM was significantly increased and that of NGT was significantly decreased. T2DM is reportedly an independent predictor for the progression of hepatic fibrosis in patients with NAFLD [10]. Our data also indicated that the development of T2DM might induce the development of hepatic fibrosis in patients with NAFLD. On the other hand, however, the presence of NASH and NAFLD themselves is reportedly associated with a high risk of developing T2DM [12].

According to the clinical and physiological data of the four groups of patients with NAFLD (Table 1), age, aspartate aminotransferase, hepatic fibrosis markers, and ferritin were higher and platelets were lower in accordance with the progression of hepatic fibrosis, as previously reported [8,23]. To clarify the

Table 4. Comparison of variable parameters of continuous glucose monitoring between patients with mild fibrosis (F0–2) and severe fibrosis (F3–4).

Variable	Mild fibrosis (F0-2)			Severe fibrosis (F3-4)			P value
Average median blood glucose (mg/dl)	108.1	±	12.2	131.5	±	34.3	<0.00001
Average standard deviation (mg/dl)	17.4	±	5.2	39.7	±	17.8	0.0022
Minimum blood glucose (mg/dl)	81.7	±	28.7	72.5	±	26.4	0.9221
Maximum blood glucose (mg/dl)	118.8	±	12.5	237.5	±	65.1	0.0019
ΔMin–max blood glucose (mg/dl)	115.2	±	22.8	165.0	±	69.6	0.0029

Average median blood glucose: average median glucose of the patients during the 24-hour monitoring period.
Average standard deviation: average standard deviation of blood glucose of the patients during the 24-hour monitoring period.
Minimum and maximum blood glucose values: lowest and highest values, respectively, during the 24-hour monitoring period.
ΔMin–max blood glucose: difference between minimum and maximum blood glucose. Data are expressed as median ± standard deviation.
doi:10.1371/journal.pone.0076161.t004

detailed glucose impairment related to the progression of hepatic fibrosis, we evaluated the various parameters of glucose metabolism. HbA1c was gradually elevated with the progression of hepatic fibrosis (Fig. 2A). Although HbA1c in the patients with F3 fibrosis was higher than that in the patients with F0 fibrosis, HbA1c in all fibrosis groups was around 6.0% because the glucose impairment in all patients in this study was mild enough to perform the 75gOGTT. On the other hand, 1,5-AG remarkably gradually decreased in accordance with the progression of hepatic fibrosis (Fig. 2B). Considering both the results of HbA1c and those of 1,5-AG, evaluation of 1,5-AG might more closely reflect the glycemic variability in patients with NAFLD, and glycemic variability would be closely related to the progression of hepatic fibrosis. IR is considered to be one of the most important predictive factors for the development of NAFLD and NASH [11]. Therefore, evaluation of HOMA-IR also was investigated in our study. HOMA-IR also gradually increased in accordance with the progression of hepatic fibrosis (Fig. 2C). However, the insulinogenic index, the ability of early insulin secretion, was not significantly different among the groups (Fig. 2D).

We next investigated and evaluated the clinical features of 75gOGTT in patients with NAFLD in relation to the progression of hepatic fibrosis (Fig. 3). After oral glucose loading, glucose levels were increased in the patients with advanced fibrosis (F3) compared with the patients with mild fibrosis (F0–2) (F3 versus F0, $P<0.01$; F3 versus F1, $P<0.001$; F3 versus F2, $P<0.05$ at 60 minutes) (Fig. 3A). The elevation of glucose levels continued until 120 minutes after oral glucose loading in the patients with F3 fibrosis. In addition, the AUC–PG as the marker for total glucose secretion after oral glucose loading also significantly gradually increased in accordance with the progression of hepatic fibrosis (F0 versus F2, $P<0.05$; F0 versus F3, $P<0.01$; F1 versus F, $P<0.05$; F2 versus F3, $P<0.05$) (Fig. 3B). Furthermore, f-IRI was significantly elevated in accordance with the progression of hepatic fibrosis (F0 versus F2, $P<0.05$; F0 versus F3, $P<0.05$; F1 versus F2, $P<0.05$; F1 versus F3, $P<0.001$) (Fig. 3C). These results are agreement with the results in Figure 2C. After oral glucose loading, insulin secretion was relatively quickly elevated in all groups of patients with NAFLD. Insulin secretion levels at 30 minutes were not statistically different among the groups. This result is in agreement with the results of the insulinogenic index (Fig. 2D). The insulin secretion in the mild fibrosis group (F0 and F1) decreased relatively early with the decrease in blood glucose levels. On the other hand, insulin secretion in the advanced fibrosis groups continued until 120 minutes. Therefore, the insulin levels at 120 minutes were remarkably higher in the patients with advanced hepatic fibrosis (F0 versus F2, $P<0.05$; F0 versus F3, $P<0.01$; F1 versus F2, $P<0.01$; F1 versus F3, $P<0.01$), as previously reported [24,25]. Furthermore, the AUC-IRI was also significantly increased in accordance with the progression of hepatic fibrosis (F0 versus F3, $P<0.05$; F1 versus F3, $P<0.01$) (Fig. 3D). It is known that insulin has the potential to function as a growth factor. IR and/or T2DM reportedly may accelerate the progression of NASH through lipogenesis, inflammation, and fibrogenesis [26] and induce cancer growth [27]. Kaji et al. also reported that not only glucose and insulin alone, but also a combination of the two, stimulated the proliferation and activation of hepatic stellate cells. They concluded that the IR status directly accelerates the development of hepatic fibrosis and hepatocarcinogenesis through activation of hepatic stellate cells [28]. Taken together with our results, hyperinsulinemia and hyperglycemia might be related to the progression of hepatic fibrosis in NAFLD.

To elucidate the predictive factors that are associated with the development of hepatic fibrosis in NAFLD, various parameters of glucose metabolism were compared between the mild fibrosis group (F0–2) and severe fibrosis group (F3). In univariate analysis (Table 2), age ($P=0.00967$), body mass index ($P=0.01395$), HbA1c ($P=0.0452$), f-IRI ($P=0.00012$), HOMA-IR ($P=0.0032$), AUC-IRI ($P=0.00103$), and AUC-PG ($P=0.01093$) were significantly higher and 1,5-AG ($P=0.00014$) was significantly lower in the severe fibrosis group than in the mild fibrosis group (Table 1, Figs. 2 and 3). As determined by multivariate logistic regression analysis, only 1,5-AG ($P=0.008$; Z value, −2.65; OR, 0.89509; 95% CI, 0.82473–0.97145) remained as the independently associated factor for advanced fibrosis (Table 3). As mentioned in the above results, it was considered that 1,5-AG might have reflected the glycemic variability in patients with NAFLD in this study.

To confirm the relationship between glycemic variability and progression of hepatic fibrosis in NAFLD, the changes in blood glucose levels during 24 hours were monitored by the CGMS in the patients with NAFLD with severe fibrosis (F3–4, $n=10$) and mild fibrosis (F0–2, $n=10$). CGMS examinations were performed at the inpatient center of Kochi Medical School, and the timing of meals and calories contained in the meals were strictly standardized during the examination. In this study, the severe fibrosis group (F3–4, $n=10$) included three patients with LC (F4) who were all diagnosed with T2DM and whose hyperglycemia was too high to perform the 75gOGTT. However, none of the patients in this study took any anti-diabetic drugs or insulin injections. Figure 4 shows that the variability of the median glucose levels of the patients with mild fibrosis (F0–2) was remarkably smaller than that of the patients with severe fibrosis (F3–4). Furthermore, the standard deviation in severe fibrosis (39.7±17.8 mg/dl) was much larger than that in mild fibrosis (17.4±5.2 mg/dl, $P=0.0022$) (Table 4). Although the minimum blood glucose levels in patients with severe fibrosis tended to be lower than those in patients with mild fibrosis (72.5±26.4 versus 81.7±28.7 mg/dl, $P=0.9221$), the maximum blood glucose level in patients with severe fibrosis was remarkably higher than that in patients with mild fibrosis (237.5±65.1versus 118.8±12.5 mg/dl, $P=0.0019$) (Table 4). As a result, the ΔMin–max blood glucose was also significantly larger in severe fibrosis than in mild fibrosis (165.0±69.6 versus 115.2±22.8 mg/dl, $P=0.0029$). The shadowed areas, which indicate glucose levels, were statistically different between the mild and severe fibrosis groups showed postprandial hyperglycemia, and the hyperglycemias were long continued (Fig. 4). Moreover, we noticed a specific clinical feature of postprandial hyperglycemia in patients with NAFLD. The peaks of postprandial hyperglycemia occurred 1 hour after every meal. Interestingly, glucose levels from midnight to early morning tended to be lower in patients with severe fibrosis and had become elevated by breakfast. The statistical differences in these parameters between the mild and severe fibrosis groups did not change even when three patients with LC (F4) were excluded from the severe fibrosis group (Figure S1 and Tables S2 and S3 in File S1). Moreover, in chronic hepatitis C, even in liver cirrhosis, the changes in blood glucose didn't necessarily show any certain patterns unlike NAFLD (data not shown). Taken together with our results, severe variability of blood glucose changes might be closely related to the progression of hepatic fibrosis in NAFLD.

Postprandial hyperglycemia and glycemic variability are reportedly involved in the progression of atherosclerosis through an increase in oxidative stress, activation of inflammatory cytokines and inflammation [13–15], and induction of other pathogenic complications [29,30,31]. In addition, repetitive postprandial glucose fluctuation reportedly evokes more pronounced adhesion of monocytes to endothelial cells compared with

that induced by stable hyperglycemia [32]. In addition, the main mechanism of monocyte adhesion to endothelial cells has been shown to be increased serum adrenaline induced by postprandial glucose spikes [33]. Furthermore, the importance of glucose variability was recently recognized as an independent factor associated with increasing mortality in patients with diabetes [34,35] and critically ill patients [36,37]. Oxidative stress is well known as one of most important factors for inflammation and progression of hepatic fibrosis in NAFLD [16,17]. Taken together with our results, therefore, variability of blood glucose might also induce monocyte adhesion to endothelial cells, activate inflammatory cytokines and inflammation, and increase oxidative stress in the liver of patients with NAFLD.

There are several limitations of this study. We showed that the prevalence of patients with T2DM was significantly increased (Fig. 1) and age and BMI tended to increase (Table 1) in accordance with the progression of hepatic fibrosis. It is known that age and BMI contribute to both the prevalence of T2DM and the progression of hepatic fibrosis. Therefore, not only progression of T2DM, but also age and BMI, might have influenced the progression of hepatic fibrosis in this study.

In conclusion, we clarified that hyperinsulinemia and hyperglycemia are important predictive factors for the development of hepatic fibrosis in this study. More importantly, variability of blood glucose is one of most important predictive factors in glucose impairment for progression of hepatic fibrosis in NAFLD. Therefore, we might need to reconsider the use of anti-diabetic drugs to inhibit the progression of hepatic fibrosis during treatment of patients with NAFLD.

Supporting Information

File S1 Supplemental Figures and Tables. Figure S1, Twenty-four-hour sensor glucose profiles by continuous glucose monitoring system. The changes in the median sensor glucose levels during 24 hours are shown in the patients with A) F0–2 fibrosis ($n = 10$) and B) F3 fibrosis ($n = 7$). The variability of median glucose levels among the patients with F0–2 fibrosis was remarkably smaller than that among the patients with F3 fibrosis. Median glucose levels in the patients with F3 fibrosis were higher than those with F0–2 fibrosis (shadows areas, $P<0.05$ to $P<0.001$): Time of meal consumption. **Table S1, Comparison of the clinical and physiological characteristics between the patients with mild fibrosis (F0–2) and severe fibrosis (F3–4).** Data are expressed as median ± standard deviation. BMI, body mass index; AST, aspartate aminotransferase; ALT, alanine aminotransferase; GGT, gamma-glutamyl transpeptidase; ChE, cholinesterase; T-Cho, total cholesterol; TG, triglycerides; FPG, fasting plasma glucose; Plt, platelets; Fe, plasma iron; HA, hyaluronic acid; IV collagen 7S, type IV collagen 7S; P-3-P, type III procollagen N-peptide. **Table S2, Comparison of the clinical and physiological characteristics between the patients with F0–2 fibrosis and F3 fibrosis.** Data are expressed as median ± standard deviation. BMI, body mass index; AST, aspartate aminotransferase; ALT, alanine aminotransferase; GGT, gamma-glutamyl transpeptidase; ChE, cholinesterase; T-Cho, total cholesterol; TG, triglycerides; FPG, fasting plasma glucose; Plt, platelets; Fe, plasma iron; HA, hyaluronic acid; IV collagen 7S, type IV collagen 7S; P-3-P, type III procollagen N-peptide. **Table S3, Comparison of variable parameters of continuous glucose monitoring between patients with F0–2fibrosis and F3 fibrosis.** Average median blood glucose: average median glucose of the patients during the 24-hour monitoring period. Average standard deviation: average standard deviation of blood glucose of the patients during the 24-hour monitoring period. Minimum and maximum blood glucose values: lowest and highest values, respectively, during the 24-hour monitoring period ΔMin–max blood glucose: difference between minimum and maximum blood glucose. Data are expressed as median ± standard deviation.
(DOCX)

Acknowledgments

Contributions: All listed authors contributed intellectually to the work presented here either through study concept and design, data acquisition, data analysis and interpretation, critical revision of the manuscript for important intellectual content; statistical analysis; funding or study supervision.

Author Contributions

Conceived and designed the experiments: MO HH Y. Ikeda KC TS. Performed the experiments: MH MO HH Y. Ikeda RY Y. Ishikawa Y. Nagata K. Munekage TO AH Y. Nozaki-Fujimura NO. Analyzed the data: K. Masuda SN NS. Wrote the paper: MH MO.

References

1. Matteoni CA, Younossi ZM, Gramlich T, Boparai N, Liu YC, et al (1999) Nonalcoholic fatty liver diseases: a spectrum of clinical and pathological severity. Gastroenterology 116: 1413–1419.
2. Rafiq N, Bai C, Fang Y, Srishord M, McCullough A, et al (2009) Long-term follow-up of patients with nonalcoholic fatty liver. Clin Gastroenterol Hepatol 7: 234–238.
3. Ono M, Saibara T (2006) Clinical features of nonalcoholic steatohepatitis in Japan: evidence from literature. J Gastroenterol 41: 725–732.
4. Reddy SK, Steel JL, Chen HW, DeMateo DJ, Cardinal J, et al (2012) Outcomes of curative treatment for hepatocellular cancer in nonalcoholic steatohepatitis versus hepatitis C and alcoholic liver disease. HEPATOLOGY 55: 1809–1819.
5. Chitturi S, Abeygunasekera S, Farrell GC, Holmes-Walker J, Hui JM, et al (2002) NASH and insulin resistance: Insulin hypersecretion and specific association with the insulin resistance syndrome. HEPATOLOGY 35: 373–379.
6. Marchesini G, Bugianesi E, Forlani G, Cerrelli F, Lenzi M, et al (2003) Nonalcoholic fatty liver, steatohepatitis, and the metabolic syndrome. HEPATOLOGY 37: 917–923.
7. Angulo P (2002) Nonalcoholic fatty liver disease. N. Engl. J. Med. 18: 1221–1231.
8. Neuschwander-Tetri BA, Clark JM, Bass NM, Van Natta ML, Unalp-Arida A, et al (2010) Clinical, laboratory and histological associations in adults with nonalcoholic fatty liver disease. HEPATOLOGY 52: 913–924.
9. Fracanzani AL, Valenti L, Bugianesi E, Andreoletti M, Colli A, et al (2008) Risk of severe liver disease in nonalcoholic fatty liver disease with normal aminotransferase levels: a role for insulin resistance and diabetes. HEPATOLOGY 48: 792–798.
10. Hossain N, Afendy A, Stepanova M, Nader F, Srishord M, et al (2009) Independent predictors of fibrosis in patients with nonalcoholic fatty liver disease. Clin. Gastroenterol. Hepatol. 7: 1224–1229.
11. Sonsuz A, Basaranoglu M, Bilir M, Turk H, Akin P (2002) Hyperinsulinemia in nondiabetic, both obese and nonobese patients with nonalcoholic steatohepatitis. Am. J. Gastroenterol. 97: 495.
12. Angulo P (2007) Obesity and nonalcoholic fatty liver disease. Nutr. Rev. 65: S57–63.
13. Ceriello A, Esposito K, Piconi L, Ihnat MA, Thorpe JE, et al (2008) Oscillating glucose is more deleterious to endothelial function and oxidative stress than mean glucose in normal and type 2 diabetic patients. Diabetes. 57: 1349–1354.
14. Node K, Inoue T (2009) Postprandial hyperglycemia as an etiological factor in vascular failure. Cardiovasc Diabetol. 8: 23.
15. Monnier L, Mas E, Ginet C, Michel F, Villon L, et al (2006) Activation of oxidative stress by acute glucose fluctuations compared with sustained chronic hyperglycemia in patients with type 2 diabetes. JAMA. 295: 1681–1687.
16. Hirose A, Ono M, Saibara T, Nozaki Y, Masuda K, et al (2007) Angiotensin II type 1 receptor blocker inhibits fibrosis in rat nonalcoholic steatohepatitis. HEPATOLOGY. 45: 1375–1381.
17. Fujii H, Kawada N (2012) Inflammation and fibrogenesis in steatohepatitis. J Gastroenterol. 47: 215–225.
18. Klonoff DC (2005) Continuous glucose monitoring: roadmap for 21st century diabetes therapy. Diabetes Care. 28: 1231–1239.

19. Bialasiewicz P, Pawlowski M, Nowak D, Loba J, Czupryniak L (2009) Decreasing concentration of interstitial glucose in REM sleep in subjects with normal glucose tolerance. Diabetic Medicine. 26: 339–344.
20. Whalan DJ (1975) The ethics and morality of clinical trials in man. Med. J. Aust. 19: 491–494.
21. Brunt EM (2001) Nonalcoholic steatohepatitis: definition and pathology. Semin Liver Dis 21: 3–16.
22. Koschinsky T, Heinemann L (2001) Sensors for glucose monitoring: technical and clinical aspects. Diabetes/Metabolism Research and Reviews 17: 113–123.
23. Yoneda M, Fujii H, Sumida Y, Hyogo H, Itoh Y, et al (2011) Japan Study Group of Nonalcoholic Fatty Liver Disease. Platelet count for predicting fibrosis in nonalcoholic fatty liver disease. J Gastroenterol. 46: 1300–1306.
24. Kimura Y, Hyogo H, Ishitobi T, Nabeshima Y, Arihiro K, et al (2011) Postprandial insulin secretion pattern is associated with histological severity in non-alcoholic fatty liver disease patients without prior known diabetes mellitus. J Gastroenterol Hepatol. 26: 517–522.
25. Manchanayake J, Chitturi S, Nolan C, Farrell GC (2011) Postprandial hyperinsulinemia is universal in non-diabetic patients with nonalcoholic fatty liver disease. J Gastroenterol Hepatol. 26: 510–516.
26. Ota T, Takamura T, Kurita S, Matsuzawa N, Kita Y, et al (2007) Insulin resistance accelerates a dietary rat model of nonalcoholic steatohepatitis. Gastroenterology. 132: 282–293.
27. Starley BQ, Calcagno CJ, Harrison SA (2010) Nonalcoholic fatty liver disease and hepatocellular carcinoma: a weighty connection. HEPATOLOGY. 51: 1820–1832.
28. Kaji K, Yoshiji H, Kitade M, Ikenaka Y, Noguchi R, et al (2008) Impact of insulin resistance on the progression of chronic liver diseases. Int J Mol Med. 22: 801–808.
29. Kilpatrick ES, Rigby AS, Atkin SL (2006) The effect of glucose variability on the risk of microvascular complications in type 1 diabetes. Diabetes Care. 29: 1486–1490.
30. Hirsch IB, Brownlee M (2005) Should minimal blood glucose variability become the gold standard of glycemic control? J Diabetes Complications. 19: 178–181.
31. Kilpatrick ES, Rigby AS, Atkin SL (2010) For debate. Glucose variability and diabetes complication risk: we need to know the answer. Diabet Med. 27: 868–871.
32. Watada H, Azuma K, Kawamori R (2007) Glucose fluctuation on the progression of diabetic macroangiopathy–new findings from monocyte adhesion to endothelial cells. Diabetes Res Clin Pract. 77 Suppl 1: S58–61.
33. Jin WL, Azuma K, Mita T, Goto H, Kanazawa A, et al (2011) Repetitive hypoglycaemia increases serum adrenaline and induces monocyte adhesion to the endothelium in rat thoracic aorta. Diabetologia. 54: 1921–1929.
34. Monnier L, Colette C (2008) Glycemic Variability. Should we and can we prevent it? Diabetes Care. 31, suppl 2: S150–154.
35. Ceriello A, Inta MA (2010) Glycaemic variability: A new therapeutic challenge in diabetes and the critical care setting. Diabetes UK. Diabetic Medicine. 27: 862–867.
36. Egi M, Bellomo R, Stachowski E, French CJ, Hart G (2006) Variability of blood glucose concentration and short-term mortality in critically ill patients. Anesthesiology. 195: 244–252.
37. Pisarchik AN, Pochepen ON, Pisarchyk LA (2012) Increasing blood glucose variability is a precursor of sepsis and mortality in burned patients. PLoS One. 7: e46582.

Transgenic Res
DOI 10.1007/s11248-013-9771-y

ORIGINAL PAPER

Aromatase-null mice expressing enhanced green fluorescent protein in germ cells provide a model system to assess estrogen-dependent ovulatory responses

Katsumi Toda · Yoshihiro Hayashi · Atsuko Yamashita · Masaru Okabe · Masafumi Ono · Toshiji Saibara

Received: 30 May 2013 / Accepted: 15 November 2013

Abstract Enhanced green fluorescent protein (EGFP) has provided us with valuable approaches for tracking living cells. We established a novel line of transgenic mice, which express EGFP in the testis and ovary. Histological analysis demonstrated that spermatids in the testis and oocytes in ovarian follicles beyond preantral stages were positive for EGFP. By exploiting these features, we evaluated ovulatory responses of aromatase-gene (*Cyp19a*) knockout mouse expressing the EGFP transgene, which is totally anovulatory due to 17β-estradiol (E2) deficiency. Ovulation in the knockout mice was induced by sequential injections of E2 on days 1, 4 and 5, pregnant mare serum gonadotropin on day 4 and human chorionic gonadotropin on day 6. Fluorescent oocytes were readily detectable at 15 h after the last gonadotropin injection in the oviduct under a fluorescence stereomicroscope, even when only one oocyte was present. However, when E2 supplementation on day 4 or day 5 in the regimen was omitted, no ovulated oocytes were detected, indicating that exogenous E2 supplementation at the time of gonadotropin stimulation is necessary to induce ovulation in aromatase-gene knockout mice. Our results further demonstrated that the current mouse line can provide an alternative tool to study germ cell biology, including oogenesis, ovulation and senescence.

Keywords Aromatase-knockout mouse · Ovulation · Estrogen · Enhanced green fluorescent protein

K. Toda (✉)
Department of Biochemistry, School of Medicine, Kochi University, Nankoku, Kochi 783-8505, Japan
e-mail: todak@kochi-u.ac.jp

Y. Hayashi
Department of Pathology, School of Medicine, Kochi University, Nankoku, Kochi 783-8505, Japan

A. Yamashita · M. Okabe
Genome Information Research Center, Research Institute for Microbial Diseases, Osaka University, Yamadaoka 3-1, Suita, Osaka 565-0871, Japan

M. Ono · T. Saibara
Department of Gastroenterology and Hepatology, School of Medicine, Kochi University, Nankoku, Kochi 783-8505, Japan

Published online: 22 November 2013

Introduction

Ovulation is a vital step for natural reproductive activity in females. It is well established that the ovulatory process is regulated by various hormones and signaling molecules (Richards 1994; Barnett et al. 2006; Drummond and Fuller 2012). We noted during ovulatory stimulation experiments that oocytes released from the ovary were not always localized in the ampulla of the oviduct. Furthermore, inaccurate estimations of ovulatory efficacy might occur when genetically manipulated mice with ovulatory impairment were employed in studies. An aromatase-deficient mouse, in which estrogen synthesis is impaired (Fisher et al. 1998; Toda et al.

2001), is such a mutant mouse with ovulatory impairment. Mouse models that facilitate detection of the ovulatory responses are highly supportive of the quantitative assessment of such responses. Enhanced green fluorescent protein (EGFP) has been used as a genetically encoded fluorescence marker owing to its autocatalytic formation of the chromophore (Tsien 1998). This protein has provided us with valuable approaches in live cell imaging, including the tracking of GFP-labeled living cells in tissues. In fact, we generated a mouse line expressing EGFP in an estrogen-dependent manner in restricted tissue sites (Toda et al. 2004) and employed it as a biosensor to assess the estrogenic activity of endocrine-disturbing chemicals (Toda et al. 2005). During the generation of EGFP-mouse lines showing expression patterns different from the previous line, a few transgenic lines were selected owing to their characteristic expression of EGFP, namely, expression of the transgene in oocytes in females. Here, we report characterization of one of the transgenic mouse lines that we obtained and its application for evaluation of the ovulatory responses of aromatase-deficient mice.

Materials and methods

Animal care

Animal experiments were carried out according to the guidelines of institutional animal regulations. All animals were maintained on a 12 h light/dark cycle at 22–25 °C and given water and phytoestrogen-low rodent chow (NIH-07PLD, Oriental Yeast Ltd., Tokyo, Japan) ad libitum. The aromatase gene (*Cyp19a*) was disrupted by homologous recombination (Toda et al. 2001). The genetic background for the present study was a mixture of C56BL/6j and BDF1.

Generation and selection of EGFP transgenic mice

The structure of the EGFP transgene employed in the present study was schematically presented in Fig. 1a. The transgene (2 kbp) consists of the estrogen-responsive element (ERE) of the Xenopus laevis A2 vitellogenin gene and a minimal promter of the mouse heat shock protein (HSP) 68 gene linked to the EGFP coding sequence and SV40 polyadenylation sequence. A DNA fragment containing the ERE (underlined in the sequence), 5′-TCTAGAGGTCACAGTGACCTGAA GTTAATGTAACCTCATCTAGA-3′ was prepared by digestion of pERETKLuc plasmid DNA (a gift from Prof. MG Parker) (Mak et al. 1999) with *Xba*I. The fragment was inserted into *Eco*RV/*Nde*I-digested pnestinhsp68EGFP (Kawaguchi et al. 2001). Transgenic mice were generated according to the method as described (Hogan et al. 1994). A purified DNA fragment obtained by digestion of the transgene vector with *Sal*I and *Sca*I was injected into fertilized eggs of a mouse strain, BDF1, which was generated by crossing between female C57BL/6 and male DBA/2. The manipulated eggs were transferred into foster mothers. A total of 59 pups (34 male and 25 female pups) were obtained. The 59 founders were outcrossed with C57BL6/J to yield F1 offspring. Transmission of the transgene was examined by PCR analysis using tail DNA with the following primers: P1-EGFP, 5′-GAGCTGGACGGCGACGT AAAC-3′; and P2-EGFP, 5′-CACCTTGATGCCGTT CTTCTGC-3′ (Toda et al. 2004), and the expression of EGFP was determined by observation of tissues from the F1 offspring under a fluorescence stereomicroscope. These analyses identified 12 founders that transmitted a functional EGFP gene. Mice of the selected line were crossed repeatedly with mice heterogeneous for the *Cyp19a* locus to produce aromatase (*Cyp19a*)-deficient mice carrying the EGFP transgene. In this report, we hereafter refer to the wild-type mice with the EGFP transgene and mice lacking the functional *Cyp19a* with the transgene as $Ar^{+/+}$ mice and $Ar^{-/-}$ mice, respectively.

Total genomic Southern blot analysis and copy number estimation of the EGFP gene

Genomic DNA (20 μg) from the tail of mouse line C41 was cleaved to completion with either *Bam*HI or *Pst*I and electrophoresed on a 0.8 % agarose gel. The DNA fragments were then transferred to a nylon membrane filter and the filter was hybridized with the ^{32}P-radiolabeled cDNA fragment coding for EGFP. In order to estimate copy numbers of the transgene integrated into the mouse genome, the coding region of the EGFP gene was amplified by PCR with P1-EGFP and P2-EGFP primers using the genomic DNA of the transgenic mouse and known amounts of the transgene used for microinjection. The amounts of the PCR products from the tail DNA were compared to those from known amounts of the transgene to calculate approximate copy numbers in the genome.

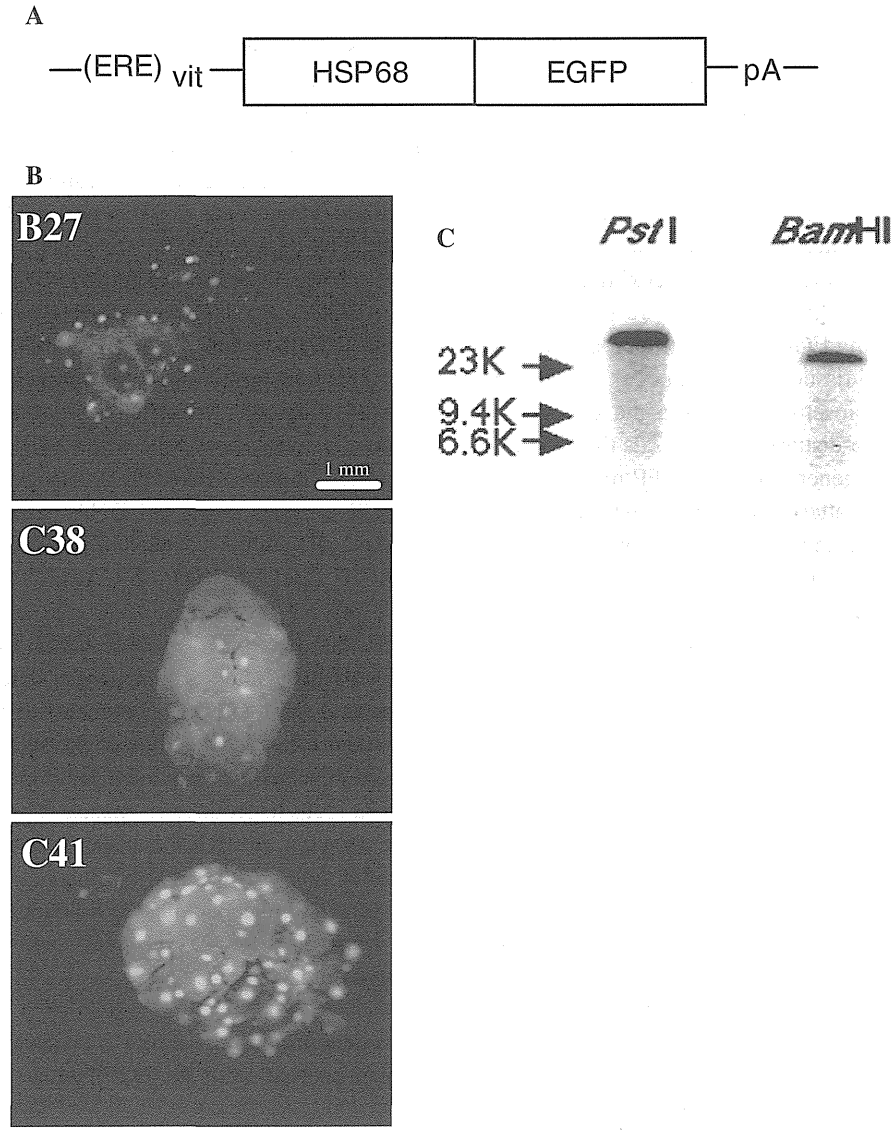

Fig. 1 Schematic view of the transgene, ovarian expression of the transgene and Southern blot analysis of the genomic DNA of the generated transgenic mice. **a** The transgene (2 kbp) consists of the estrogen-responsive element of the Xenopus leavis A2 vitellogenin gene and a minimal promoter of the heat shock protein 68 gene (HSP68) linked to the EGFP cDNA (EGFP) and SV40 polyadenylation sequence (pA). **b** Assessment of EGFP expression in the ovary of three founder lines in vivo. Imaging of EGFP fluorescence was performed with a fluorescence stereomicroscope for the unfixed ovary. *Scale bar* is 1 mm. **c** Total genomic Southern blot analysis on mouse of line C41. Genomic DNA from $Ar^{+/+}$ mice with the EGFP gene was digested completely with either *Pst*I or *Bam*HI. A radiolabeled fragment of cDNA coding for EGFP was used as a probe

Visualization and recording of EGFP fluorescence

Imaging of EGFP fluorescence was carried out using a fluorescence stereomicroscope (MZ FLIII; Leica, Deerfield, NJ) with a filter set, composed of a 480/440-nm excitation filter and a 510-nm barrier filter. The images were recorded using a cooled digital color charge-coupled device camera (C4742-95, Hamamatsu Photonics, Hamamatsu, Japan) mounted on the stereomicroscope.

To obtain images of EGFP fluorescence in sections, ovary and testis were fixed in a solution of 4 % (v/v)

paraformaldehyde at 4 °C for 1 h and then immersed in phosphate-buffered saline containing 10 % (w/w) sucrose at 4 °C for 15 h. The tissues were embedded in optimal cutting temperature compound (Sakura, Tokyo Japan) and cut into 15-μm-thick sections. After DNA was stained with 4,6-diamidino-2-phenylindole·2HCl (DAPI), sections were observed under a fluorescence microscope (Olympus BX50, Olympus, Tokyo Japan).

Quantification of EGFP fluorescence

To prepare tissue extracts containing EGFP, tissues (~0.2 g) from five transgenic mice for each genotype at 2-month-old were homogenized in 2 ml of 10 mM Tris–HCl (pH 7.2) containing 1 mM EDTA and 0.2 % (w/w) sodium dodecyl sulfate using a Polytron PT1200 homogenizer (KINEMATICA, Lucerne, Switzerland). After centrifugation at 2,000×*g* for 10 min at 4 °C, the supernatants containing EGFP were recovered for fluorometry using a spectrofluorometer (RF-5300PC, Shimadzu Corp., Kyoto, Japan). The filters used were 480 nm for excitation and 510 nm for emission. Purified recombinant EGFP (BD Clontech, Palo Alto, CA, USA) was employed as a standard to calibrate the amounts of EGFP expressed in the tissues of the transgenic mice (Toda et al. 2004). The amounts of EGFP in the extracts are expressed as picograms of EGFP per microgram of total protein of the tissue extracts examined.

Induction of ovulation

Powder (15 mg) of 17β-estradiol (E2) (Sigma, minimum 96 % purity) was first dissolved in 0.8 ml of ethanol, then diluted to 8 ml with sesame oil (Nacalai Tesque, Kyoto, Japan). Pregnant mare serum gonadotropin (PMSG) (Serotropin®, ASKA Pharmaceutical Co., Ltd., Tokyo, Japan) and human chorionic gonadotropin (hCG) (Wako Pure Chemical Industries, Osaka, Japan) were dissolved in 0.9 % NaCl solution at 500 and 2,500 international units (IU)/ml, respectively. Ovulatory induction was conducted according to a protocol described previously (Toda et al. 2012) with slight modifications. In Group A, $Ar^{-/-}$ mice at 4 weeks of age were supplemented with E2 on days 1, 4 and 5 (18 mg/kg body weight, subcutaneous injection). In Groups B, C, and D, E2 supplementation on day 1, day 4, and day 5 was, respectively, omitted (Table 2). The mice were injected with PMSG (25 IU/mouse, intraperitoneal injection) on day 4. At 48 h after PMSG injection (on day 6), hCG (25 IU/mouse, intraperitoneal injection) was administered. $Ar^{+/+}$ mice were stimulated with 5 IU of PMSG and hCG on day 4 and day 6, respectively. Ovulatory response was observed under a fluorescence stereomicroscope at 15 h after the hCG injection.

Statistical analysis

Data are expressed as the mean ± SEM. The significance of differences was analyzed by unpaired *t* test using InStat software (GraphPad Software, Inc., San Diego, CA, USA). *P* values less than 0.05 were considered significant.

Results

Generation and selection of transgenic mice expressing EGFP protein

Twelve (7 males and 5 females) of the 59 founder lines expressed functional EGFP. Fluorescence stereomicroscopic analysis revealed that three of the 12 founders expressed the EGFP gene in oocytes (Fig. 1b). As line C41 showed the strongest fluorescence in the ovary among these three lines under a fluorescence stereomicroscope. We characterized line C41 more extensively. We noticed no impairment in fertility in line C41, producing on average 6.5 ± 1.7 offspring per litter (male, 3.2 ± 1.3; female, 3.7 ± 1.7) (n = 30 litters). Total genomic Southern blot analysis by digestion of the murine DNA with *Pst*I or *Bam*HI, of which the recognition sequence does not exist within the EGFP gene, gave a single band hybridized with the EGFP probe, suggesting that the transgene was incorporated at a single locus in the genome (Fig. 1c). Approximately 6 copies of the EGFP transgene were estimated to be incorporated into the genome when analyzed by PCR amplification.

Quantitative analysis of EGFP expression using 2-month-old mice of line C41 revealed high expression in heart and adrenal gland in both female and male mice (Fig. 2). The analysis also showed that a relatively high level of EGFP expression (more than 20 pg EGFP/μg protein) was detected in the lung and uterus in $Ar^{+/+}$ females and in the skeletal muscle,

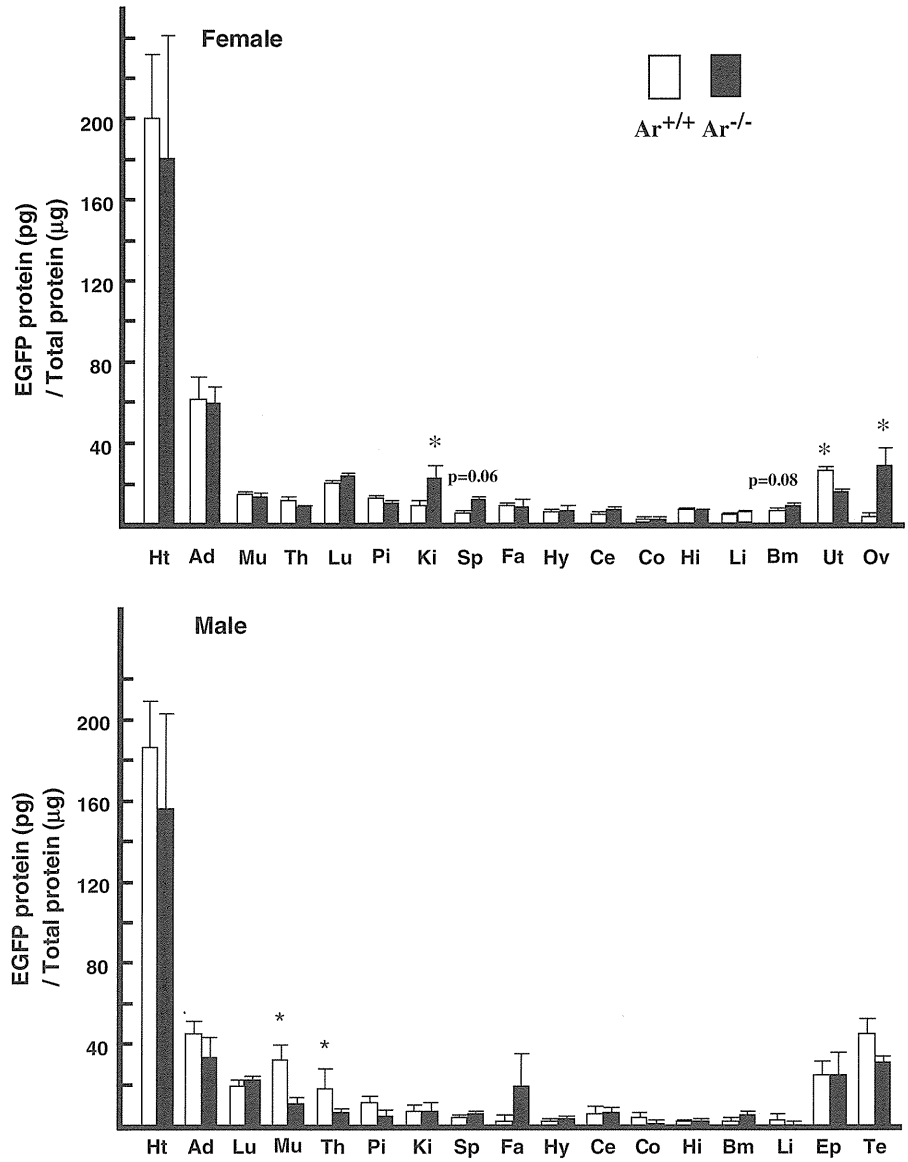

Fig. 2 Tissue distribution of EGFP in mouse of line C41. Quantitative analysis of EGFP expression using 2-month-old females (*upper panel*) and males (*lower panel*). The amounts of EGFP were measured by fluorescent spectrophotometry in various tissues including heart (*Ht*), adrenal gland (*Ad*), skeletal muscle (*Mu*), thymus (*Th*), lung (*Lu*), pituitary gland (*Pi*), kidney (*Ki*), spleen (*Sp*), gonadal fat pad (*Fa*), hypothalamus (*Hy*), cerebellum (*Ce*), cortex (*Co*), hippocampus (*Hi*), liver (*Li*), bone marrow (*Bm*), uterus (*Ut*), ovary (*Ov*), epididymis (*Ep*) and testis (*Te*) The amounts are expressed as pg EGFP per μg total protein for each tissue examined. The analysis was carried out on five animals per group. Open and closed bars indicate $Ar^{+/+}$ and $Ar^{-/-}$ mice, respectively. $*P < 0.05$ relative to $Ar^{-/-}$ mice fed a control chow diet. The *error bars* represent the SEM

epididymis and testis in $Ar^{+/+}$ males. Low levels of the EGFP expression (<20 pg/μg protein) were detected in the other several tissue sites examined (Fig. 2). Quantification of EGFP expression in the females of lines B27 and C38 showed high levels of expression in heart and adrenal gland as observed in line C41 (Table 1). We also detected high levels of EGFP expression in the kidney, fat pad, liver and ovary in females of line B27, but the expression level in the lung and uterus was not marked as observed in line C41. In contrast to lines C41 and B27, EGFP expression was generally high in all tissue examined,

Table 1 Tissue distribution of EGFP in female $Ar^{+/+}$ mice of lines B27 and C38

	Line B27	Line C38
Heart	36.1 ± 3.2	41.8 ± 9.7
Adrenal gland	43.6 ± 7.5	54.9 ± 2.6
Skeletal muscle	4.4 ± 0.5	16.1 ± 2.8
Thymus	9.8 ± 2.7	13.0 ± 3.5
Lung	12.9 ± 0.6	30.9 ± 9.0
Pituitary gland	9.9 ± 1.1	70.0 ± 15.3
Kidney	36.9 ± 4.9	64.9 ± 14.2
Spleen	9.1 ± 0.4	9.6 ± 1.0
Fat pad	28.4 ± 4.9	34.1 ± 4.2
Hypothalamus	15.5 ± 2.5	46.3 ± 4.9
Cerebellum	18.5 ± 0.9	35.1 ± 4.1
Cortex	14.4 ± 1.8	34.9 ± 5.5
Hippocampus	12.9 ± 1.5	35.2 ± 4.5
Liver	22.5 ± 2.6	18.9 ± 3.7
Bone marrow	9.1 ± 0.6	ND
Uterus	11.0 ± 1.9	34.6 ± 8.4
Ovary	20.2 ± 5.0	29.0 ± 2.9

The amounts were expressed as EGFP (pg) per total protein (μg) for each tissue

ND not determined

except for skeletal muscle, thymus, spleen and liver in females of line C38.

Expression of the EGFP gene in $Ar^{-/-}$ mice of line C41

The expression levels of EGFP in mice of line C41 lacking *Cyp19a* ($Ar^{-/-}$ mice) were compared to those in the $Ar^{+/+}$ mice to assess the estrogen dependence of transgene expression. High levels of expression were detected in heart, adrenal gland, lung and uterus, as observed in $Ar^{+/+}$ females. In addition, the kidney and ovary expressed the EGFP gene at high levels in $Ar^{-/-}$ females. Of these tissues, the kidney, uterus and ovary showed a significant difference compared with the expression levels in $Ar^{+/+}$ females (Fig. 2). Although not statistically significant, expression levels in the spleen and bone marrow were higher in $Ar^{-/-}$ mice than in $Ar^{+/+}$ females. In $Ar^{-/-}$ male mice, the expression was reduced in the muscle and thymus, and increased in the gonadal fat pad compared with those in the $Ar^{+/+}$ males. Whereas uterine expression of the transgene was higher in $Ar^{+/+}$ mice than in $Ar^{-/-}$ mice, the differences in the expression levels in the other tissue sites seemed to be marginal between $Ar^{+/+}$ and $Ar^{-/-}$ mice.

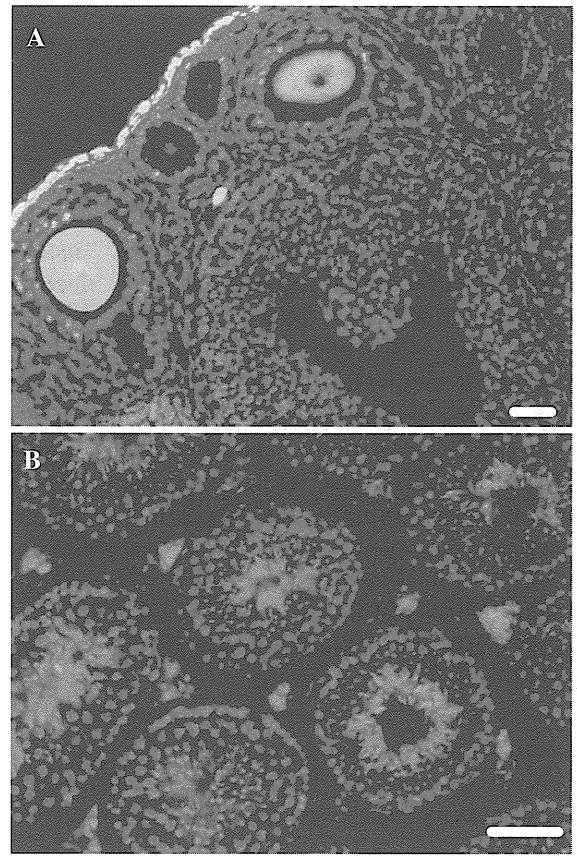

Fig. 3 Expression of the EGFP gene in the gonadal tissues of mouse of line C41. Imaging of EGFP fluorescence expressed in the $Ar^{+/+}$ ovary (**a**) and testis (**b**) was performed with a fluorescence microscope for sections of the fixed tissues. Leydig cells in the interstitial space of testis (**b**) showed non-specific fluorescence, as testicular sections of mice without the EGFP gene revealed similar fluorescent images under our experimental conditions. *Scale bar* is 100 μm

Expression of EGFP in germ cells

Next, we examined the gonadal expression of EGFP more closely in mice of line C41. The results clearly demonstrated that the expression was restricted to oocytes and was found in neither granulosa nor theca cells in the ovary. Furthermore, oocytes before preantral stages did not express the EGFP gene (Fig. 3a). Examination using testicular sections revealed that the spermatids were the cells expressing the EGFP gene.

We detected EGFP expression neither in spermatogonia, spermatocytes nor mature spermatozoa (Fig. 3b).

Ovulatory induction of mice expressing the EGFP gene

We employed the transgenic mouse line C41 to evaluate the ovulatory response of the $Ar^{-/-}$ mouse. When ovulation was induced in the $Ar^{+/+}$ mice by gonadotropin injections at standard doses (5 IU of PMSG and hCG), the fluorescent oocytes were observed in the oviducts at 15 h after hCG injection (Fig. 4a, b). As reported previously (Toda et al. 2001), when $Ar^{-/-}$ females were stimulated with the same dose of gonadotropins, no EGFP-positive oocytes were detectable in the oviducts (data not shown). In contrast, upon treatment of $Ar^{-/-}$ mice with the alternative super-ovulatory protocol (Toda et al. 2012), EGFP-positive oocytes were detected in the oviducts (Fig. 4c). These results demonstrated that the current transgenic mouse line expressing EGFP in oocytes allows us to assess ovulatory responses accurately and conclusively.

Next, we examined which E2 supplementations, given at three points within the protocol: days 1, 4 and 5, are essential for the ovulatory induction in $Ar^{-/-}$ mice. Ovulatory response could be detected in five out of twelve $Ar^{-/-}$ mice examined after the treatment without the E2 supplementation on day 1 (Table 2). In contrast, when the supplementation on day 4 ($n = 11$) or on day 5 ($n = 14$) was omitted, no $Ar^{-/-}$ mice showed ovulation, indicating that E2 supplementation after gonadotropin stimulation is essential for ovulatory induction in $Ar^{-/-}$mice.

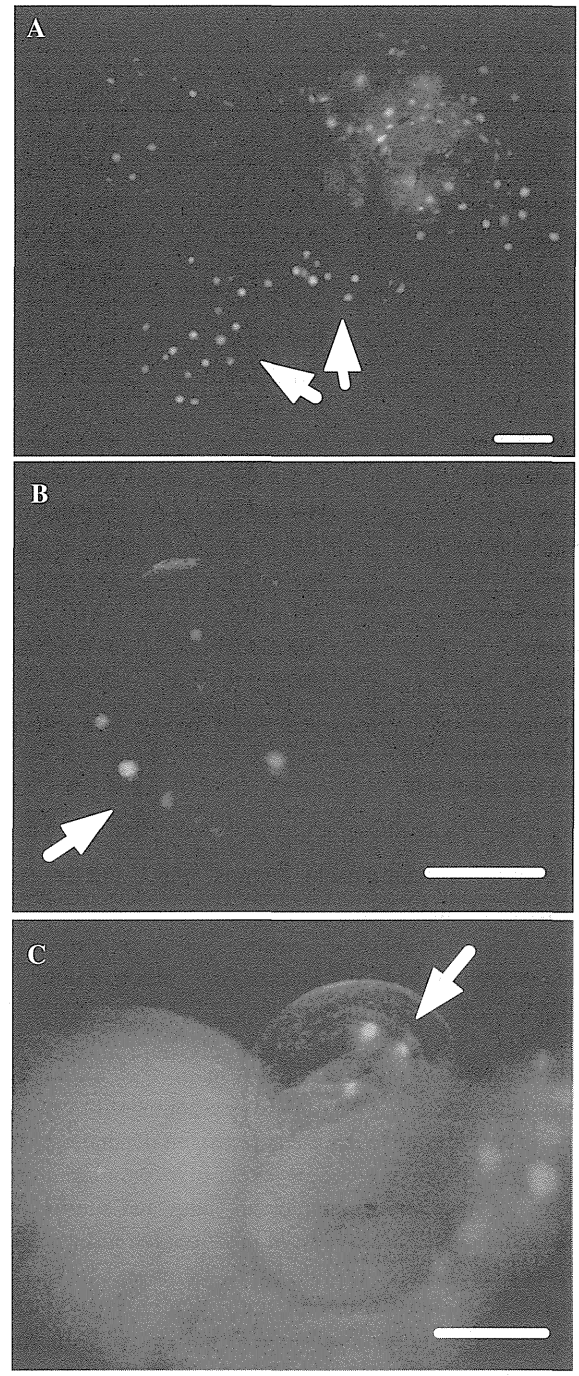

Fig. 4 Ovulated oocytes in the oviducts observed with a fluorescence stereomicroscope. In $Ar^{+/+}$ (**a**, **b**) and $Ar^{-/-}$ females (**c**) of line C41 at 4 weeks of age, ovulation was induced. Ovulatory responses were evaluated under a fluorescent stereomicroscope at 15 h after the hCG injection. *Arrows* indicate ovulated oocytes expressing EGFP. *Scale bar* is 0.5 mm

Discussion

The EGFP transgenic mouse line C41 was fortuitously generated. Southern blot analysis using total genomic DNA of the present transgenic mouse suggested that the transgene is integrated at a single unique site in the genome. Comparison of the abundance of EGFP fluorescence between $Ar^{+/+}$ and $Ar^{-/-}$mice of line C41 revealed that the uterine expression was higher in the former mice than in the latter, indicating that the expression seems to be estrogen-dependent. However, we detected higher expression of the transgene in the

Table 2 Ovulatory response of $Ar^{-/-}$ mice

	Day 1	Day 4		Day 5	Day 6	Number of mice examined	Number of mice ovulated	Number of oocytes ovulated	Reference
	E2 (18 mg/kg)	E2 (18 mg/kg)	PMSG (25 IU)	E2 (18 mg/kg)	hCG (25 IU)				
Group A	+	+	+	+	+	60	42	6.9 ± 0.9	Toda et al. (2012)
Group B	−	+	+	+	+	12	5	4.4 ± 1.1	This study
Group C	+	−	+	+	+	11	0	–	This study
Group D	+	+	+	−	+	14	0	–	This study

ovary in the $Ar^{-/-}$ mice than that in $Ar^{+/+}$ mice. Furthermore little differences in the expression levels in the pituitary gland, which is highly sensitive to estrogenic chemicals (Toda et al. 2005), were observed between 2-month-old $Ar^{+/+}$ and $Ar^{-/-}$mice. We thus concluded that the EGFP transgene in line C41 was expressed in an estrogen-independent manner in vivo. Shedding of the estrogen-dependency might be caused by silencing the function of the regulatory element due to genomic integration of the transgene (Ristevski 2005). It is also tempting to speculate that some regulatory networks of gene expression have become functional in heart, adrenal gland and germ cells due to the influence of regulatory elements neighboring the integration site of the transgene. Nevertheless, quantitative analysis of EGFP expression showed high levels of its expression in heart and adrenal gland in three different founder lines, indicating that the transcriptional controlling units including the DNA fragment containing the ERE of the Xenopus leavis A2 vitellogenin gene and the transcription driving sequence from the mouse HSP68 gene might preferentially promote the expression of the EGFP gene in the tissue sites.

Histological analysis of gonadal tissues of line C41 revealed the expression of EGFP in spermatids in the testis and oocytes in ovarian follicles beyond preantral stages. We did not observe the expression in spermatogonia nor in oocytes in primordial follicles. Thus the expression of the EGFP transgene in line C41 might depend on factor(s) that might get to be functional after the germ cells progress to a certain stage of development. We also observed no EGFP expression in spermatozoa present in the lumen of seminiferous tubules or epididymis. The negative expression in spermatozoa seems to be due to removal of cytoplasm during a process of development of compact and slender spermatozoa from spermatids.

It was reported that the expression of EGFP in vivo negatively correlates with the developmental competence of preimplantation mouse embryos (Devgan et al. 2004) and also affects metabolic activities (Li et al. 2013). Current transgenic mouse line C41 did not reveal a detectable sign of reproductive difficulty. Nevertheless the litter size was smaller than that of our previous EGFP reporter, line KT2 (Toda et al. 2004), showing on average 8.9 ± 2.2 offspring per litter (n = 19 litters). This might reflect some detrimental effects of EGFP expression in oocytes on reproductive activity. However the differences in the litter size might be attributable to differences in the genetic background between the two lines.

Genetically modified murine models such as mice lacking the SULT1E1 gene (Gershon et al. 2007) or LRH-1 gene (Duggavathi et al. 2008) demonstrated that ovarian estrogens at high levels were detrimental to ovulatory induction. In order to elucidate the minimum requirements of E2 supplementations for ovulatory induction in aromatase-deficient mice, we employed $Ar^{-/-}$ mice of line C41, in which fluorescent oocytes are readily detectable within the oviduct, allowing us to evaluate accurately the ovulatory responses after stimulation with various combinations of stimulants including E2. The results demonstrated an absolute requirement of E2 supplementation at the time when gonadotropins were administered for ovulatory induction in $Ar^{-/-}$ mice. It is well established that luteinizing hormone receptor (LH/CG-R) expression was induced by synergic actions of E2 and FSH (Richards et al. 1979; Knecht et al. 1985). We confirmed the synergism in aromatase-deficient mice as well (Toda et al. 2012). It is thus interesting to examine whether or not different protocols for E2 supplementation can alter the synergic actions of E2 with FSH for LH/CG-R expression in $Ar^{-/-}$ mice, which might explain the observed differences in the

ovulatory responses in $Ar^{-/-}$ mice. Furthermore, recent studies employing microarray analysis identified a number of estrogen-dependent genes in the murine ovary (Liew et al. 2011; Binder et al. 2013). Expression analysis on those ovarian genes under the present experimental conditions using $Ar^{-/-}$ mice might be able to delineate a novel set of ovulation-related genes induced by synergic action of E2 and FSH.

In summary, various studies characterized mouse lines that harbor a reporter transgene in germ cells (Zambrowicz et al. 1993; MacGregor et al. 1995; Yeom et al. 1996; Lewandoski et al. 1997; Vidal et al. 1998; Yoshimizu et al. 1999; de Vries et al. 2000; Han et al. 2004; Lan et al. 2004; Nayernia et al. 2004; Tanaka et al. 2004; Cronkhite et al. 2005; Payer et al. 2006; Gallardo et al. 2007; West et al. 2009; Nicholas et al. 2009). Of these lines, some reporters have limitations in that they are sex-specific (Zambrowicz et al. 1993; Vidal et al. 1998; Nayernia et al. 2004) and/or may be limited in expression to the early stages of germ cell differentiation (MacGregor et al. 1995; Tanaka et al. 2004). The current transgenic mice expressed EGFP in germ cells at later stages of differentiation. We exploited this advantage to investigate the ovulation of $Ar^{-/-}$ mice, which are totally anovulatory (Fisher et al. 1998; Toda et al. 2001), demonstrating that our current EGFP transgenic mouse provides an alternative tool to study germ cell biology, including oogenesis, ovulation and senescence.

Acknowledgments We thank Dr. Teruhiko Okada for his contributions to the study at its early stage. This study was supported in part by a Grant-in-Aid for Scientific Research from the Ministry of Education, Culture, Sports, Science and Technology, Japan, to T. Saibara (No. 24590981) and K. Toda (No. 25460315).

References

Barnett KR, Schilling C, Greenfeld CR, Tomic D, Flaws JA (2006) Ovarian follicle development and transgenic mouse models. Hum Reprod Update 12:537–555

Binder AK, Rodriguez KF, Hamilton KJ, Stockton PS, Reed CE, Korach KS (2013) The absence of ERβ results in altered gene expression in ovarian granulosa cells isolated from in vivo preovulatory follicles. Endocrinology 154:2174–2187

Cronkhite JT, Norlander C, Furth JK, Levan G, Garbers DL, Hammer RE (2005) Male and female germline specific expression of an EGFP reporter gene in a unique strain of transgenic rats. Dev Biol 284:171–183

de Vries WN, Binns LT, Fancher KS, Dean J, Moore R, Kemler R, Knowles BB (2000) Expression of Cre recombinase in mouse oocytes: a means to study maternal effect genes. Genesis 26:110–112

Devgan V, Rao MRS, Seshagiri PB (2004) Impact of embryonic expression of enhanced green fluorescent protein on early mouse development. Biochem Biophys Res Commun 313:1030–1036

Drummond AE, Fuller PJ (2012) Ovarian actions of estrogen receptor-β: an update. Semin Reprod Med 30:32–38

Duggavathi R, Volle DH, Mataki C, Antal MC, Messaddeq N, Auwerx J, Murphy BD, Schoonjans K (2008) Liver receptor homolog 1 is essential for ovulation. Genes Dev 22:1871–1876

Fisher CR, Graves KH, Parlow AF, Simpson ER (1998) Characterization of mice deficient in aromatase (ArKO) because of targeted disruption of the cyp19 gene. Proc Natl Acad Sci USA 95:6965–6970

Gallardo T, Shirley L, John GB, Castrillon DH (2007) Generation of a germ cell-specific mouse transgenic Cre line, Vasa-Cre. Genesis 45:413–417

Gershon E, Hourvitz A, Reikhav S, Maman E, Dekel N (2007) Low expression of COX-2, reduced cumulus expansion, and impaired ovulation in SULT1E1-deficient mice. FASEB J 21:1893–1901

Han SY, Xie W, Kim SH, Yue L, DeJong J (2004) A short core promoter drives expression of the ALF transcription factor in reproductive tissues of male and female mice. Biol Reprod 71:933–941

Hogan B, Beddington R, Costantini F, Lacy E (1994) Manipulating the mouse embryo: a laboratory manual, 2nd edn. Cold Harbor Laboratory, Cold Spring Harbor

Kawaguchi A, Miyata T, Sawamoto K, Takashita N, Murayama A, Akamatsu W, Ogawa M, Okabe M, Tano Y, Goldman SA, Okano H (2001) Nestin–EGFP transgenic mice: visualization of the self-renewal and multipotency of CNS stem cells. Mol Cell Neurosci 17:259–273

Knecht M, Brodie AMH, Catt KJ (1985) Aromatase inhibitors prevent granulosa cell differentiation: an obligatory role for estrogens in luteinizing hormone receptor expression. Endocrinology 117:1156–1161

Lan Z-J, Xu X, Cooney AJ (2004) Differential oocyte-specific expression of Cre recombinase activity in GDF-9-iCre, Zp3cre, and Msx2Cre transgenic mice. Biol Reprod 71:1469–1474

Lewandoski M, Wassarman KM, Martin GR (1997) Zp3–cre, a transgenic mouse line for the activation or inactivation of loxP-flanked target genes specifically in the female germ line. Curr Biol 7:148–151

Li H, Wei H, Wang Y, Tang H, Wang Y (2013) Enhanced green fluorescent protein transgenic expression in vivo is not biologically inert. J Proteome Res. doi:10.1021/pr400567g

Liew SH, Sarraj MA, Drummond AE, Findley JK (2011) Estrogen-dependent gene expression in the mouse ovary. PLoS ONE 6:e14672

MacGregor GR, Zambrowicz BP, Soriano P (1995) Tissue non-specific alkaline phosphatase is expressed in both embryonic and extraembryonic lineages during mouse embryogenesis but is not required for migration of primordial germ cells. Development 121:1487–1496